Temperature Estimation in Trailer Disc Brake

Sofia Finnved

Sebastian Nöbbelin

LUND UNIVERSITY

Department of Automatic Control

MSc Thesis
ISRN LUTFD2/TFRT--5966--SE
ISSN 0280-5316

Department of Automatic Control
Lund University
Box 118
SE-221 00 LUND
Sweden

Printed in Sweden by Tryckeriet i E-huset
Lund 2015

Sammanfattning

Automatiska bromsfunktioner i lastbilar och bilar kan rädda liv, men de kan även höja temperaturen i bromsarna till farligt höga nivåer. Olika alternativ för temperaturmodellering i skivbromsar har utvärderats i rapporten. De har gemensamt att temperaturen är homogen i bromsskivan och det antagandet ger bra resultat. Implementationen av modellerna är gjord i Simulink.

En av modellerna uppskattar uppvärmningen i bromsen beroende på hur stor skillnad i kinetisk energi som bromsningen ger upphov till. Hur stor del av energiändringen som beror på rull- och luftmotstånd, och hur stor del som beror på arbetet som bromsarna utför, är svårt att uppskatta. Dessutom inverkar förarens körsätt i vissa fall. Detta faktum gör modellen mindre lämplig att använda i det generella fallet. Mer lovande sätt att modellera uppvärmningen på utgår ifrån lufttrycket i bromscylindern. Detta lufttryck omvandlas till en bromskraft på olika sätt, som har sina respektive fördelar och nackdelar. Gemensamt för dem är att massan över hjulaxeln måste vara känd, och i rapporten utgås det ifrån att den är det. En förenklad, exponentiell avsvalning ger tillräckligt bra resultat. Avsvalningen modellerad som konvektion och strålning ger ännu bättre resultat.

Bromskraftsmodellen användes för en undersökning av jämviktstemperaturer vid pulsbromsning av skivbromsen. Inga säkra slutsatser dras från undersökningen men resultaten är lovande. De pekar mot att en fortsatt utveckling av en pulsbromsande säkerhetsfunktion är möjlig.

Abstract

Automatic brake functions in trucks and cars can save lives but may heat the brakes to dangerous temperature levels. Various types of models for temperature estimation in a disc brake have been evaluated. A homogeneous temperature inside the disc was assumed and this simplification gave adequate modeling results. The implementation was done in Simulink.

One model estimated the heat generation based on the kinetic energy difference during a brake event. The difficulty of estimating driving resistance coefficients and the sensitivity to the driver's behavior made this model less suitable for generalization. More promising models used the brake cylinder pressure as input. The brake cylinder pressure was used to derive a braking force at the periphery of each wheel. The braking force could be determined in different ways, each one with their own advantages and disadvantages. The common disadvantage was that the brake force depends on the load over each wheel. It was assumed that the load over each wheel be known. A simple, exponential model for cooling gave sufficiently good results. A model based on the sum of convection and radiation gave better results.

The brake pressure model was used in a short study on steady state temperatures, while the vehicle was pulse braked. No conclusions was drawn from these simulations, but the results were promising, thus opening up for future research.

Acknowledgements

First of all, we would like to express our gratitude to our supervisors: Professor Rolf Johansson at Lund University (department of Automatic Control), Jenny Gahlin and Thomas Strange at Scania, who have contributed with great assistance and guidance. Without your excellent feedback and assistance along the way, the thesis would never have been completed.

Many more have contributed with assistance during our work at Scania. We would especially like to thank Martin Edinger, Niklas Kanders, Xavier Dreux and Martin Sundberg at Scania for valuable discussions, help with measurement setup and truck driving assistance.

Last but not least, we are very grateful to our respective families and friends that have been by our side and supported us during our study period at Lund University.

To all, thank you!

List of Variables

Variable	Description	Unit
A_f	Projected frontal area.	m^2
A_s	Area subjected to convection and radiation.	m^2
a_v	Vehicle deceleration due to braking.	$m\ s^{-2}$
B	Dynamic tire radius.	m
b	Cooling coefficient.	s^{-1}
B_i	Biot number, constant expressing the ratio between the heat transfer resistance on the surface and inside a body.	-
C_d	Aerodynamic drag coefficient.	-
C_p	Specific heat capacity.	$J\ K^{-1}$
D	Effective brake diameter.	m
F	Force.	N
F_1	Force created by the brake chamber.	N
F_{air}	Air resistance force.	N
F_{brake}	Braking force between the pad and the disc.	N
F_{dec}	Total decelerating force of the trailer.	N
F_{drive}	Modelled driving resistance.	N
F_θ	Driving resistance force from the road inclination.	N
F_w	Decelerating force at the periphery of a trailer wheel.	N
g	Gravitational constant.	$m^3\ kg^{-1}\ s^{-2}$
h	Convective heat transfer coefficient.	$W\ m^{-2}\ K^{-1}$
i	Mechanical enhancement of the force F_1.	-
k	Conductive heat transfer coefficient.	$W\ m^{-1}\ K^{-1}$
m_d	Mass of the brake disc.	kg
M_{dec}	Decelerating moment caused by braking.	N m
m_t	Trailer mass.	kg

m_v	Mass of the vehicle.	kg
m_w	Mass supported by a wheel.	kg
N	Number of wheels braking the vehicle combination.	-
p_c	Constant brake pressure needed to avoid jackknife behavior.	Bar
P_m	Control line air pressure to trailer.	Bar
p_p	Pulsed brake pressure needed to avoid jackknife behavior.	Bar
$\dot{Q}_{conv}$	Time derivative of convection energy.	J s^{-1}
Q_{drive}	Work done by driving resistance.	J
$\dot{Q}_{drive}$	Time derivative of work done by the drive resistance force.	J s^{-1}
Q_{in}	Energy input into the disc.	J
$\dot{Q}_{in}$	Time derivative of energy input into the brake.	J s^{-1}
Q_{ke}	Kinetic energy.	J
$\dot{Q}_{ke}$	Time derivative of kinetic energy.	J s^{-1}
Q_{out}	Energy output from disc	J
$\dot{Q}_{out}$	Time derivative of energy output from the brake.	J s^{-1}
$\dot{Q}_{rad}$	Time derivative of radiation energy.	J s^{-1}
r	Significant length for a body, for example radius.	m
r_{brake}	Effective brake radius.	m
R_{roll}	Roll resistance force.	N
T	Brake temperature.	K
T_{amb}	Ambient temperature around the brake.	K
T_i	Initial temperature.	K
t_{stop}	Duration for a coast-down test.	s
v	Velocity.	m s^{-1}
v_{init}	Initial velocity during a coast-down test.	m s^{-1}
v_v	Vehicle velocity.	m s^{-1}
v_{wind}	Wind velocity.	m s^{-1}
W	Work.	J
x	Design parameter used to convert the control line brake pressure to brake cylinder pressure.	Bar
z	Braking rate.	-
ε	Emissivity for a surface.	-
η	Mechanical efficiency of the disc brake system.	-

θ	Road gradient.	rad
μ	Friction coefficient between the brake pad and the disc brake.	-
ρ	Density of Air.	kg m^{-3}
σ	Stefan-Boltzmann constant.	W m^{-2} K^{-4}
φ	Accelerometer signal measuring the road inclination.	m s^{-2}
ω	Angular velocity of the disc brake.	rad s^{-1}

List of Figures

List of Tables

Contents

1

Introduction

1.1 Motivation

Driving a heavy duty vehicle with a trailer combination in hilly terrain that could be wet, icy or with lots of turns, have always been a subject of danger for the driver. One reason being the increased risk of the so called jackknife effect. The jackknife effect occurs when the trailer pushes the towing vehicle around until it hits the trailer, see Fig. 1.1 on p. 2. The stability is lost, the vehicle combination folds, and there is nothing the driver can do to continue the journey. Jackknifing can also be a danger for other road users, mainly because the driver of the heavy duty vehicle loses control of the vehicle. A solution to counteract jackknifing should increase the safety for the driver and the fellow road users. Such a function, that could predict and stabilize the heavy duty vehicle before the jackknifing occurs, could save lives.

Trucks using an Electronic Brake System (EBS) have the capabilities of controlling the trailer brake pressure separately. To deflect situations where the trailer is pushing the towing vehicle, it would be possible to brake the trailer with a low brake pressure for a short time, stabilizing the combination. This could however, if often used, create high temperatures in the brake system due to the heat generation from friction. If the brake system is heated above its limit, the brake pads start to *fade* and the braking power may be effected negatively. Loss of friction in service brakes due to too high temperatures is called fading.

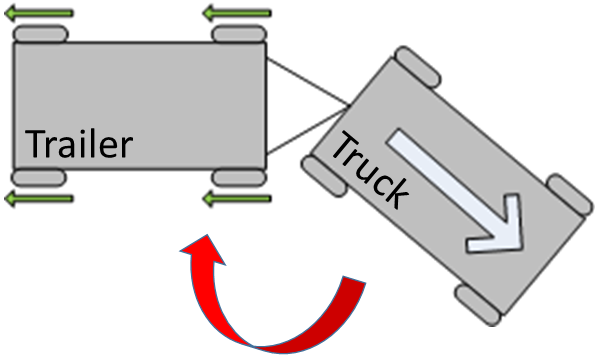

Figure 1.1 Jackknifing, the movement indicated by the curved arrow, is a dangerous situation that should be avoided. A small brake pressure acting on the trailer, the small arrows in the figure, could stabilize the vehicle combination.

1.2 Problem Description

It is of interest to model the temperature build-up and cooling to ensure that the function explained above is safe, both for the driver and the other road users. The temperature model has to be robust to handle different vehicle and trailer combinations. It shall, for example, be able to handle the inputs:

- trailer brake pressure,
- vehicle combination velocity,
- ambient temperature,
- slope of the road

and return the temperature as the output in discrete time. For a given temperature limit, the model shall also be able to supply the stability brake function with information whether it could be active or not. The model shall estimate the temperature with an accuracy of $\pm$ 50 °C. The emphasis in this thesis is to find a model estimating the temperature in the disc brake and to investigate the maximum temperature achieved while pulse braking the trailer to obtain vehicle stability at a certain velocity.

1.3 Limitations

To achieve the scope of this master's thesis it is preferable to simplify the model as much as possible. Therefore, only disc brake systems will be investigated and the disc brake will be assumed to be a homogeneous body with a uniform temperature.

1.4 Outline

The report is organised in 7 main chapters. The theoretical background is presented in Chap. 2 and includes basic knowledge about the disc brake system, a thermodynamic temperature modeling approach and the basic thermodynamics needed to understand the work. Chap. 3 explains how the experimental data was acquired and what methods were used to create the temperature estimation models. Furthermore, in Chap. 4, the results are presented. In Chap. 5, the modeling approach and the various parts of the models are discussed, as well as the equipment used. The second last chapter, Chap. 6, summarises the thesis. The final chapter, Chap. 7, gives an outline of future improvements of the work made in this thesis.

1.5 Contribution by Authors

Both authors have been involved in all parts of the master's thesis.

2

Theory

This chapter presents the theory on which the thesis is founded. The chapter includes a basic introduction to the disc brake system, a thermodynamic temperature modeling approach and the thermodynamics needed to understand the problem.

2.1 Brake Systems

In this section the disc brake system is described, and the differences between disc brakes and drum brakes will be mentioned. These are the two types of service brake systems used by heavy duty vehicle and trailer combinations. A short explanation of the auxiliary brakes will follow.

Disc Brakes

Disc brake systems are not isolated well from the environment. The consequence of this is that a lot of dirt particles may get into the system and impair the mechanisms or cause the system to wear down faster by abrasion [Fransson, 2009]. This could be hazardous in extreme environments, for example in a mine.

The positive aspect of having an open system is that a lot of air may flow inside and around the disc brake. With a lot of air flow, the cooling of the disc is more efficient.

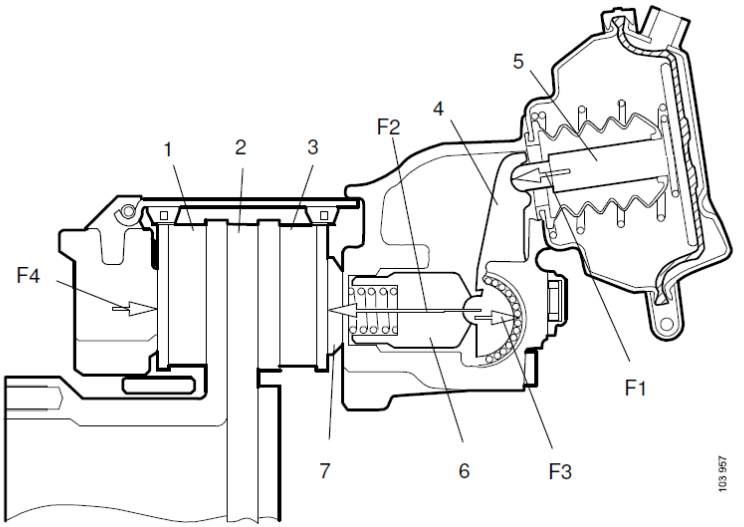

Figure 2.1 Cross section of the complete disc brake system.

The disc brake system consists of a ventilated brake disc, a floating disc brake caliper and a brake cylinder controlled by compressed air. The complete disc brake system is visualized by the cross section schematics seen in Fig. 2.1:

1. Outer brake pad
2. Brake disc
3. Inner brake pad
4. Lever arm
5. Pressure bar
6. Adjustable mechanism
7. Piston

The disc brake system is activated by a pressure from the brake cylinder acting as a force F_1 onto the lever arm. The lever arm reacts by creating a force F_2 on the adjustable mechanism which transfer this force through the piston onto the inner brake pad. This in return creates a counteracting force F_3 in the opposite direction.

Since the caliper is floating, a force F_4 is created acting onto the outer brake pad. Both brake pads are therefore pressed against the brake disc. Due to friction, a negative moment decreasing the rotational velocity of the wheel is created [*10-00 Bromskunskap* 2015].

Drum Brakes

Instead of a *disc* brake system, a *drum* brake system can be used. The disc is, here, exchanged with a drum, which the brake pads are pressed outwards against in order to decelerate the vehicle combination. The drum brake system is therefore more shielded against particles, given the isolated structure of the drum, which also results in worse thermal properties. The heat produced inside the drum brake is not cooled as effective as the disc brake by the surrounding air.

Auxiliary Brakes

Together with the service brakes, Scania vehicles have two additional means to reduce vehicle speed; the retarder and the exhaust brake. These brakes are intended to unburden the service brakes. Both to prolong the time until the brakes are worn out and to prevent the risk of overheating and potential fading.

Simplified, the hydraulic retarder uses vanes enclosed in a chamber on the power-train, after the clutch. Filling it with oil, the vanes will be slowed down depending on how much oil is pumped into the chamber and the vehicle will be decelerated. The exhaust brake works by closing the exhaust pipe, compressing the exhaust gases. This will counteract the engine and slow it down, effectively braking the vehicle.

2.2 Modeling Approaches

Heat generation in the disc brake is produced by reducing the kinetic energy by braking, forcing the brake pads to retard the wheel through friction. Friction braking produces a lot of heat and the disc absorbs 99% of the energy while the rest is absorbed by the brake pads [Day et al., 2012].

In [Sheridan et al., 1988], four different approaches for temperature modeling was presented with increasing complexity. Two of them are estimating temperatures in 2-D and 3-D via the Finite Difference method and the Finite Element method, respectively. Due to their long computation time, these cannot be implemented in real time in a vehicle and are therefore outside the scope of this master's thesis. An analytic one-dimensional model estimating the surface temperature of the brake disc is also described. The simplest analytical model presented is a zero-dimensional lumped capacitance model which will be explained in more detail below.

2.3 Lumped Capacitance Model

The simplest approach is to model the disc as a piece of gray iron with uniform temperature; the lumped capacitance model [Lienhard IV and Lienhard V, 2011]. This model seems to be the most commonly used method when temperature estimation is done for continuous braking in disc brakes or as in [Naji and AL-Nimr, 2001], in drum brakes. In [Nisonger et al., 2011], this is showing good results for disc brakes on a race car. For this simplification to be valid, the conduction of heat within the disc has to be much higher than the convection of heat energy from the disc to the surrounding air. This validation can be done through computation of

$$\mathrm{B}_i = \frac{hr}{k} \tag{2.1}$$

in which B_i is the dimensionless *Biot number*, h the convective heat transfer coefficient, k the conductive heat transfer coefficient and r the critical dimension of which conduction occurs, in this case the disc radius. If $\mathrm{B}_i < 0.1$ is fulfilled; the lumped capacitance model is relevant and is sufficient for modeling the temperature.

For a lumped capacitance model, the temperature difference in the disc is related to a change in internal energy:

$$m_d C_p \frac{dT}{dt} = \dot{Q}_{in} - \dot{Q}_{out} \tag{2.2}$$

in which m_d is the disc mass, C_p the heat capacity, dT/dt the change in temperature, $\dot{Q}_{in}$ the generated heat flux into the disc and $\dot{Q}_{out}$ the dissipation heat flux out of the disc. The heat fluxes $\dot{Q}_{in}$ and $\dot{Q}_{out}$ may be modeled in different ways. The following sections will further delve into the modeling approaches of the heat fluxes.

2.4 Heat Generation

The heat flux into the disc is produced through the friction-based brake system. When the brakes are applied with a pressure, the brake pads will press towards the disc. Through friction, the disc rotational speed will be decreased and heat is generated by the brake system [Hwang et al., 2008]. The braking process can also be seen as a force working to decelerate the vehicle. The work W expended by a force F is for velocity v:

$$W = \int F v dt \tag{2.3}$$

This gives one way to model the heat generation through the relationship [Talati and Jalalifar, 2009]:

$$\dot{Q}_{in} = F_{brake} v_v \tag{2.4}$$

in which F_{brake} is the force at the contact area between the brake pad and the brake disc due to friction and v_v the vehicle velocity. Rewriting Eq. 2.4 gives:

$$\dot{Q}_{in} = F_{brake} r_{brake} \omega \tag{2.5}$$

in which r_{brake} is the effective radius from the center of the brake disc to the brake pad and ω the angular velocity of the brake disc.

Brake Force Formula

The deceleration of a wheel may be determined through mechanical modeling of the brake system seen in Fig. 2.1. A simplification of the disc brake system is seen Fig. 2.2.

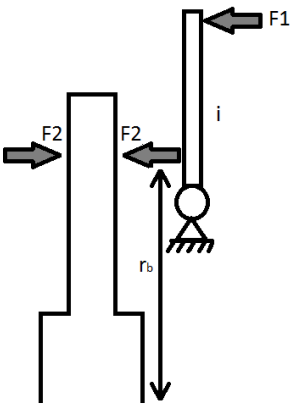

Figure 2.2 Simplified disc brake system.

The force that pushes the pads against the disc brake causes a decelerating moment through friction. This moment depends on the force created by the brake chamber, F_1, that is enhanced by the lever arm to a force, F_2, pushing the pad against the disc. Assuming symmetry, the same force is pushing the pad on the opposite side. This allows the construction of a formula that describes the decelerating moment M_{dec}:

$$M_{dec} = 2F_2 r_{brake} = 2F_1 i\mu\eta r_{brake} = F_1 i\mu\eta D \tag{2.6}$$

where i is the internal ratio of which the force F_1 is enhanced, $D = 2r_{brake}$ the effective disc diameter, μ the friction coefficient and η the mechanical brake system efficiency. The multiplication with 2 is necessary because there are two pads decelerating the brake disc with the same force. Furthermore, a brake force is derived by division with the dynamic tire radius:

$$F_w = \frac{F_1 iD\mu\eta}{B} \tag{2.7}$$

in which F_w is the braking force at the periphery of the wheel in contact with the road surface and B the dynamic tire radius. The dynamic tire radius is used since the tire is not perfectly round while driving.

Friction A vehicle brake system depends on friction forces between the pads and the disc to slow the vehicle down. This friction coefficient is highly dynamic. Spots of new surface material are created in complicated reactions between the disc and the pads and the friction coefficient varies. It is also known that the friction coefficient is affected by how the braking system has been used. If the braking system is used exceedingly, the friction increases since the surface particles are worn away. On the other hand, if the braking system is not used for a long duration of time, the friction power is decreased.

In [Fransson, 2009] it is concluded that the friction coefficient is hard to model due to its complex nature. It is seen in two identically performed tests that the resulting friction coefficient measures are completely different, which demonstrates the difficulty of a friction based model.

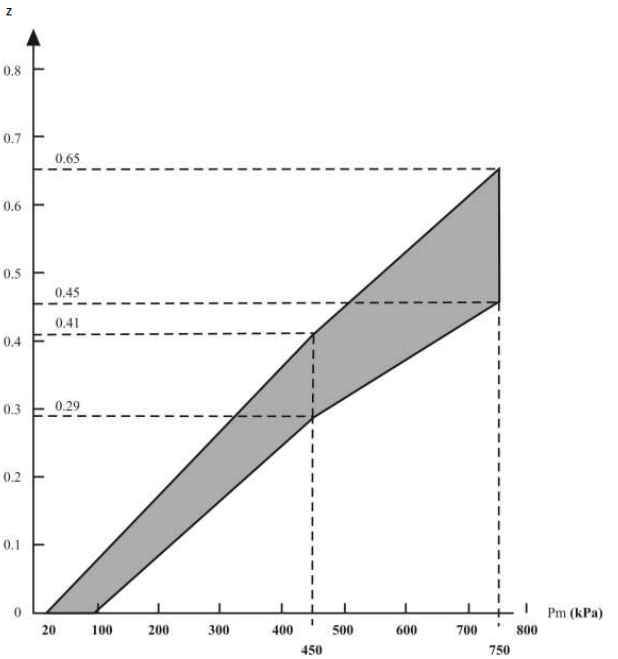

Figure 2.3 The relationship between the braking rate of the vehicle and the control line brake pressure [*Vehicle Regulations UN ECE-R13* 2008].

Brake Regulations

To assure safety on the road, the UN stands behind some regulations on brake systems. One of these regulations state that the control line brake pressure P_m, sent from the towing vehicle to the trailer, must correspond to a satisfying deceleration a_v of the vehicle combination. The control line brake pressure is determined by the driver via the brake pedal (or, for example, by an automatic safety function reacting to some external or internal events). In this report, the brake cylinder pressure is measured in Bar[1] instead of the SI unit Pa; 1 Bar = $1 \cdot 10^5$ Pa. Since every brake system differs, the deceleration from a given brake pressure varies. This depends on the characteristics and state of the brake system. However, the allowed deceleration of the vehicle combination must always be within a satisfying range. This is stated in [*Vehicle Regulations UN ECE-R13* 2008] and the regulation corresponds to a brake corridor of allowed range of deceleration or *braking rate* (see below) for a specific control line brake pressure, see Fig. 2.3. The braking rate must always be contained by the upper and lower lines. These regulations concern all vehicles in, but not limited to, the EU.

[1] This is common in the automotive industry.

The same trailer brake cylinder pressure will result in different braking rates depending on the trailer mass m_t. The current trailer mass is estimated with a mechanical or electrical sensor, attached to the trailer. This information is used to translate the control line brake pressure (the desired braking rate) to an appropriate brake cylinder pressure $(P_m - x)$, x depending on the current situation.

The braking rate is the ratio between the total braking force at the periphery of all wheels and the total normal static reaction of road surface on the trailer. Or in mathematical terms:

$$z = \frac{F_{dec}}{m_t g} \tag{2.8}$$

in which z is the braking rate, g the gravitational constant and F_{dec} the total braking force of the trailer. Therefore, multiplying the braking rate with the gravitational constant, a vehicle deceleration is derived. For a specific trailer, this knowledge can be used to estimate a minimum or maximum amount of heat flux entering the system at a certain P_m, assuming that the mass supported by the wheel is known. Reformulating Eq. 2.8, the deceleration can then be expressed as a force:

$$F_{dec} = m_t a_v = m_t z g \quad . \tag{2.9}$$

As in Eq. 2.4 on p. 8, the heat flux into the brake is theoretically

$$\dot{Q}_{in} = \frac{F_{dec} v_v}{N} = \frac{m_t a_v v_v}{N} = F_w \tag{2.10}$$

where N is the number of wheels braking the vehicle and F_w the braking force at the periphery of a wheel.

Kinetic Energy Loss

Another way to model the heat flux is to estimate the change in kinetic energy due to braking. The truck's kinetic energy Q_{ke},

$$Q_{ke} = \frac{1}{2} m_v v_v^2 \tag{2.11}$$

where m_v is the mass of the vehicle, is not only transformed to heat in the brakes when the vehicle is decelerated. According to [Hammarström et al., 2012], a lot of factors influence the kinetic energy losses except for the brakes; the *driving resistance* F_{drive} (with the gear in neutral position):

- resistance from the transmission oil,
- resistance in the wheel bearings,
- air resistance depending on the truck design and trailer type used,

- resistance from inertia,
- the slope of the road in longitudinal and lateral directions and
- rolling resistance.

In [Rajamani, 2006] the following equation

$$F_{drive} = F_{air} + \sum R_{roll} = \frac{1}{2}\rho C_d A_f (v_v + v_{wind})^2 + \sum R_{roll} \tag{2.12}$$

is used to model the driving resistance. F_{air} is the air resistance force, R_{roll} the rolling resistance force, ρ the air density, C_d the aerodynamic drag coefficient, A_f the projected frontal area of the truck, v_v the vehicle velocity and v_{wind} the wind velocity.

Additionally, the slope of the road, θ, has an influence of the amount of energy needed to decelerate the vehicle. This give rise to the drive resistance modeled as

$$F_{drive} = \frac{1}{2}\rho C_d A_f (v_v + v_{wind})^2 + \sum R_{roll} + m_v g \sin(\theta) \tag{2.13}$$

illustrated by Fig. 2.4.

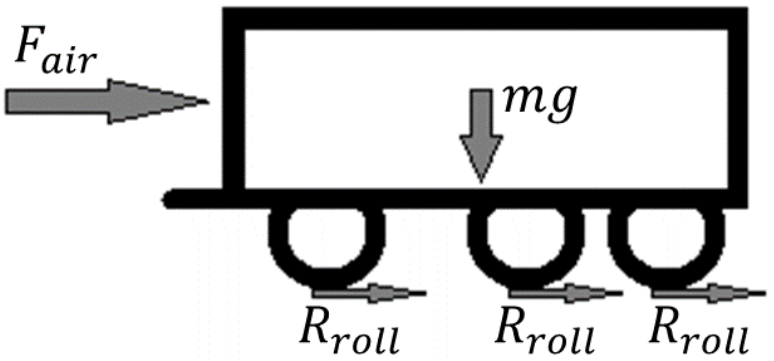

Figure 2.4 Modeled forces acting on the trailer. The air resistance F_{air}, the gravitational force $m_v g$ and the roll resistance R_{roll} acting on all wheels individually.

The work expended by the air- and roll resistance, Q_{drive}, will be

$$Q_{drive} = \int F_{drive} v_v dt \tag{2.14}$$

and since energy cannot be created or destroyed according to the law of conservation of energy [Alonso and Finn, 1980], only transformed, the energy used to heat the brakes, Q_{in}, may be estimated as

$$Q_{in} = Q_{ke} - Q_{drive} \quad . \tag{2.15}$$

This gives the estimated heat flux to the brakes as the time derivative of Eq. 2.14

$$\dot{Q}_{in} = \dot{Q}_{ke} - \dot{Q}_{drive} \tag{2.16}$$

$$= m_v v_v a_v - F_{drive} v_v \quad . \tag{2.17}$$

2.5 Heat Dissipation

The cooling of the disc depends on convection and radiation. For lower temperatures, convection is the biggest contributor to cooling. In [Shen et al., 1997], it is noted that at a temperature around 600 K the radiative heat flux has increased to 10 % of the total convective heat flux. Thus, it can be assumed that the radiative contribution with respect to convection is low.

The thermodynamical formulation of convective heat flux, $\dot{Q}_{conv}$, to the surroundings is the following:

$$\dot{Q}_{conv} = hA_s(T - T_{amb}) \tag{2.18}$$

where A_s is the active convective heat surface area, T the uniform temperature of the disc and T_{amb} the temperature of the air surrounding the disc brake system.

The radiation of the disc is as mentioned only visible at higher temperatures. The thermodynamic representation of radiative heat flux, $\dot{Q}_{rad}$, is given by:

$$\dot{Q}_{rad} = \varepsilon \sigma A_s(T^4 - T_{amb}^4) \tag{2.19}$$

where A_s is the area affected by radiation, ε the emissivity and σ the Stefan-Boltzmann constant [Bejan, 1993]. The total heat dissipation is then described by:

$$\dot{Q}_{out} = \dot{Q}_{conv} + \dot{Q}_{rad} \tag{2.20}$$

Approximation of the Cooling Coefficient

Eq. 2.18 has two parts that are hard to derive; the active convective heat surface area A_s and the convective heat transfer coefficient h. The active area is hard to derive since the disc has complex geometry. This allows air to flow inside the disc to

increase the convection to the surrounding air. The second problem is that h depends on the aerodynamic properties of the disc brake, i.e,. the flow of air passing through the disc [Limpert, 1975].

According to [Limpert, 1975], the uncertainty in modeling the temperature using the convective heat transfer coefficient h may be as big as 10-30%, why the convective cooling coefficient is better adjusted according to measured data rather than from table look up. The product of h and A_s could be parametrized together to simplify the modeling further. In [Nisonger et al., 2011] this is done through solving Eq. 2.2 on p. 7 when only convection is present:

$$\frac{dT}{dt} = -\frac{hA_s}{C_p m_d}(T - T_{amb}) \quad . \tag{2.21}$$

By assuming that C_p is constant, the solution to this differential equation is:

$$T(t) = e^{-bt}(T_i - T_{amb}) + T_{amb} \tag{2.22}$$

where T_i is the intial temperature and $b = hA_s/C_p m_d$ the *cooling coefficient* describing how fast the body is cooled. In [Kwangjin, 1999], it is motivated that the cooling coefficient depends linearly on vehicle velocity v_v, which is why it is assumed that the product h and A_s also depends linearly on vehicle velocity. This is done in [Shen et al., 1997] with as good accuracy as a much more complex finite element aerodynamical model of the disc brake. The relationship between hA_s and v_v can thus be determined through cooling measurement data for different vehicle velocities.

Heat Capacity

The solution to Eq. 2.21 assumes that the heat capacity is constant. This is however not true. In [Nisonger et al., 2011], the heat capacity dependency of temperature is presented. It is seen that the heat capacity depends linearly on the temperature in a range between 0 and 700 °C. For higher temperatures, the heat capacity becomes nonlinear. It changes because the gray iron starts to alter its material properties when heated above 740 °C [“Introduction to Gray Cast Iron Brake Rotor Metallurgy”]. The heat capacity is derived through experiments using a NETZSCH model 457 *MicroFlash*^{TM} laser flash diffusivity apparatus [Schopper, 2008]. How the experiment is conducted is left for the interested reader to look up.

With a temperature dependent heat capacity C_p, the differential equation, see Eq. 2.21, is not adequately solved. However, it is stated and showm in the literature that the cooling of the disc is exponentially decreasing. It is therefore motivated that the cooling behavior may be fitted with good accuracy to an exponentially decreasing function following Eq. 2.22. It is further motivated by [Shen et al., 1997] and [Nisonger et al., 2011] that a constant C_p can be used to give a good estimate of the product h and A_s.

3

Method

This chapter presents the methods used to derive a temperature estimation model. This includes experimental data gathering as well as how the model implementation was done. The methods used in this chapter are based on information from the theory chapter.

3.1 Experimental Data Gathering

The vehicle, both the truck and the trailer, were weighed before the data acquisition. Various tests were conducted at the test track at Scania, Södertälje. The disc brake was heated through casual driving around the test track, braking the vehicle with regular intervals, preferably when travelling downhill.

3-Axle Trailer

The trailer used is a trailer with three axles, one in the front and two in the back (a so called bogie), see Fig. 3.1. The second axle of the trailer can be raised if the axle loads allow this. The maximum total load is 27 000 kg when using all three axles.

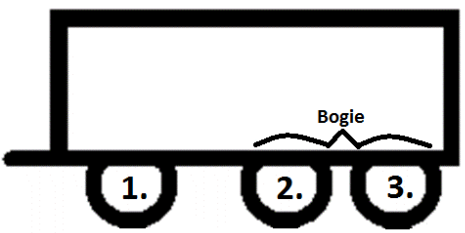

Figure 3.1 Figure illustrating the trailer used during the experimental data gathering.

Figure 3.2 The outer temperature sensor on the disc brake.

Figure 3.3 The inner temperature sensor on the disc brake.

Temperature Sensors

Before the first measurements with the trailer, two dragging temperature sensors (thermocouples, type K) were placed at two different locations on the disc. One close to the outer edge, see Fig. 3.2, and the other one close to the inner edge, see Fig. 3.3. A pressure sensor was attached to the brake cylinder. The measurements were done at the first axle, right wheel.

Between the first and the second measurements, a third thermocouple was added, intended to measure the ambient temperature close to the disc. This was placed behind the wheel axle. The reason for this was to find the spot with the worst cooling conditions possible around the brake.

3.2 Existing Data Sets

Some temperature data from previously acquired test runs were available to begin with. Unfortunately, the truck was not weighed prior to most of these measurements. This made it hard to make use of them other than as preliminary data for developing the Simulink models.

There were one temperature data gathering done previously on the 3-axle trailer. During this data gathering the second axle on the trailer , see Fig. 3.1 on p. 15, was raised. Thus, it was running on two axles only. The data was gathered while driving in and around Södertälje. The axle load was measured prior to the data gathering and the trailer disc brake temperature was measured using the same thermocouples as described in Sec. 3.1.

Before the data was gathered, several roll out tests were done. This, to derive a relationship between the deceleration due to braking and the control line brake pressure P_m. The test was done driving at a constant speed, disengaging the clutch, allowing the wheels to roll freely and then applying a constant brake pressure for some time. The deceleration while braking and rolling freely can then be derived, which allows the deceleration due to braking to be derived as the difference between them. A theoretical sketch of how this looks is seen in Fig. 3.4. At time t_1 the clutch is disengaged. At time t_2, a constant control line brake pressure is applied until time t_3. The deceleration due to braking at the specific pressure is then found as the difference between $v'_v(t), t_2 < t < t_3$ (the braking sequence) and $v'_v(t), t_1 < t < t_2$ (the rolling sequence).

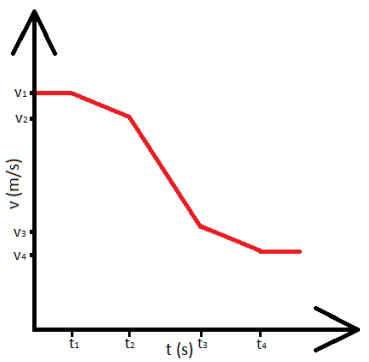

Figure 3.4 Theoretical sketch of a roll out test to determine the deceleration due to braking.

Thickness: 1.510 mm / Density: 7.169 g/cm³

Temperature /℃	Thermal Diffusivity /mm²/s	Specific Heat /J/(g·K)	Thermal Conductivity /W/(m·K)
25	15.561	0.420	46.854
101	13.556	0.453	44.024
200	11.784	0.494	41.733
300	10.336	0.527	39.050
401	9.114	0.569	37.177
501	7.976	0.632	36.138
601	6.794	0.708	34.484
701	5.344	0.844	32.335

Figure 3.5 The measured heat capacity, depending on temperature, for gray iron [Schopper, 2008].

3.3 Heat Capacity

In Sec. 2.5 it was discussed how the heat capacity depends on temperature. The measurement data is seen in Fig. 3.5 and in Fig. 3.6 on p. 19 the dependency is shown. Furthermore, in [Schopper, 2008] it is shown that the heat capacity for different gray iron compositions are roughly the same. The data were sampled from room temperature up to 900 °C with several samples each 100 °C and is seen in Fig. 3.6.

From this information it is possible to derive an equation that represent the relationship through fitting of data. Since the target function that the model is used for should not exceed high temperatures, the nonlinear transition above 700 °C can be discarded. In fact, the target area of temperature is between 0 and 500 °C. It is then possible to fit the data to a linear function between 0 and 500 °C using MATLAB's basic fitting tool.

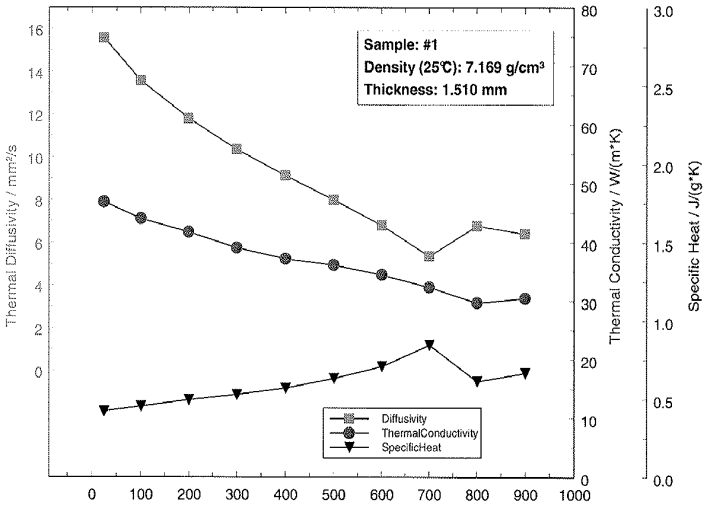

Figure 3.6 The heat capacity as a function of temperature using the data in Fig. 3.5 on p. 18.

3.4 Cooling Characteristics

Cooling Coefficient

Since the cooling coefficient, $b = hA_s/C_p m_d$, depends linearly on the velocity, it is possible to derive the relationship through experiments. This is done by heating the disc to a specific temperature and then cruise at a constant velocity for a duration of time. Through regression analysis, the cooling coefficient that is connected to the constant vehicle velocity, may be found. If this is done for multiple velocities, it is possible to determine the linear function that describes the cooling coefficient for the disc with respect to the velocity:

$$b = k_1 v_v + m_1 \tag{3.1}$$

in which k_1 and m_1 are the phenomenological [1] parameters to be derived with the experimental data. This allows the cooling characteristics to be implemented as an exponentially decreasing function.

Convective Coefficient

It is also possible to derive a model for the product hA_s, also called the convection coefficient. To do this, it is important that the sampled cooling coefficients b are

[1] Phenomenological model: A model describing the data rather than the underlying physics.

transformed to hA_s:

$$hA_s = bC_p m_w \tag{3.2}$$

where m_w is the wheel mass, before approximating it with a linear function. The initial temperature T_i is used to derive the constant heat capacity C_p used for the conversion to the convective coefficient. The resulting model for the convection coefficient is then:

$$hA_s = k_2 v_v + m_2 \quad , \tag{3.3}$$

where k_2 and m_2 are the parameters derived with the modified experimental data for the convection coefficient. This allows the convection to be implemented following Eq. 2.18 on p. 13.

Radiative Coefficient

In Eq. 2.19 on p. 13 the radiative behavior of the heat dissipation is discussed. To model the radiation through the theoretic equation, the emissivity and surface area subject to radiation has to be known. The surface area subject to radiation could be estimated through assuming that the inner complex geometry does not contribute to the cooling. This would give a rough estimate of the surface area subject to radiation. Also, the emissivity of the surface is hard to determine. For gray iron, oxidized surfaces gives a huge variation in the emissivity, which can vary anywhere between 0.6 and 0.95 [*optris CTlaser LT/1M/2M/3M/G5*]. Due to the complex nature of estimating these parameters and radiation being a small part of the cooling the product, $A_s\varepsilon$, could be estimated, reducing the complexity. The estimation of the parameters will then be done with experimental data and tweaked until the result is good.

3.5 Brake Force Model

Brake Corridor

In Sec. 2.4, the brake regulations were presented. The regulation state the maximum and minimum allowed deceleration for a given control line brake pressure P_m, see Fig. 2.3. To be implemented for a general trailer, a worst case scenario has to be assumed. For this purpose, in theory, the worst case scenario for the temperature estimation model is when the highest deceleration for a given P_m is achieved. It is however not common that a trailer brake system is at the top of the corridor, since this would wear the brakes faster, shortening its lifetime. Therefore, it is more likely that the trailer brake system is in the lower region of the brake corridor. Hence, it can be assumed that, in reality, the worst case trailer position is somewhere close to the middle of the corridor. This is a linear curve in the middle of the corridor:

$$a_v = g(P_m - x) \cdot 0.0947 \tag{3.4}$$

in which x is an adjustable conversion parameter, converting the control line brake pressure to a brake cylinder pressure through the difference $(P_m - x)$. This allows

the construction of a function mapping control line brake pressure to decelerating force through Eq. 2.9 on p. 11:

$$F_w = m_w g(P_m - x) \cdot 0.0947 \tag{3.5}$$

in which the equation holds for positive values F_w only.

The conversion parameter x varies between trailers due to pad wear and material properties. This is the reason why it is left as an adjustable variable. However, the linear curve should be somewhere in the middle of the brake corridor.

Roller Bench Test

It has been mentioned continuously throughout the report that the brake performance between trailers varies a lot. This is due to the characteristics and state of the brake systems. A newly installed brake system does not brake as effective as a brake system that is worn in. Furthermore, a brake system that has not been used for a while gives less deceleration. A method to find out the state of the brake system is the so called roller bench test. This test is used to analyze the brake force of a specific wheel axle for different control line brake pressures.

The test is carried out by putting the wheels on the axle of interest on two cylinder rolls. Pressure sensors are then applied to the control line brake pressure and the brake cylinder pressure. The measurement is initialized by rotating the cylinders and therefore the vehicle axle. By slowly increasing the control line brake pressure, the force acting on the cylinders is measured. When that force reach a maximum value (depending on the axle load), the rollers driving the axle stops and the test is finished, independent of the current control line brake pressure.

From the result, it is possible to construct a function describing the relationship from control line brake pressure to brake force:

$$F_w = k_3(P_m - m_3) \tag{3.6}$$

in which k_3 and m_3 are the parameters subject to the fitting. The equation is only valid for positive brake force values F_w.

Verification Data Set

In Sec. 3.2, a temperature data set was presented. This data set contained sufficient data to be used with the brake force model. Before the data gathering the axle load was measured. The weight of the first axle was 7710 kg, giving a weight per wheel of 3885 kg on this specific axle. It was also presented how the deceleration relationship with the control line brake pressure P_m was derived with the roll out test. The resulting data is seen in Table 3.1 on p. 22. Fitting a function to the deceleration data makes it possible to derive the decelerating force F_w using Newton's second law.

control line brake pressure P_m (Bar)	Deceleration (m/s^2)
0.00	0.00
0.50	0.00
0.60	0.10
1.00	0.54
1.50	1.02
2.00	1.52
3.00	2.53
6.00	5.50

Table 3.1 Deceleration data derived during the validation data gathering already existing on Scania.

Convective and Radiative Cooling

Using the knowledge that the disc brake is cooling exponentially, the cooling coefficient can be estimated using least-squares estimation as described in [Johansson, 2012]. The estimation is done for measurement data of the temperature, during constant velocity cruising, with regression analysis. The cooling coefficients can then be transformed into convective coefficients, as described in Sec. 3.4, knowing the initial cooling temperature and the disc mass. The convection coefficients may then be used to fit a function describing the dependency of velocity.

Furthermore, the convective coefficient is estimated with measurement data of the temperature when the vehicle is standing still. This because stand still cooling is assumed to give the smallest convective cooling coefficient. Combining this with the function describing the dependency with velocity, a complete convective cooling description is derived. The radiative cooling coefficient is estimated through measurement data as described in Sec. 3.4.

Ambient Temperature of the Disc Brake

The air surrounding the disc brake is the main contributor to reducing the temperature through convection and radiation, see Eq. 2.18 and Eq. 2.19 on p. 13. For this reason it is interesting to investigate how the ambient temperature of the disc brake varies. It depends mainly on the disc brake temperature and the vehicle velocity. However, to simplify the model, only the disc temperature will be considered. Thus, measuring the ambient temperature and the temperature of the disc, a worst case linear model can be derived.

3.6 Kinetic Energy Model

Driving resistance

A coast down test was made to find values of the parameters for the air- and roll resistance. During a coast-down test, under the assumptions of calm weather ($v_{wind} \approx 0$) and no road gradient, the vehicle is taken to some initial velocity v_{init}. Immediately, the vehicle is put in neutral gear and is allowed to roll freely until the vehicle has stopped at time t_{stop}. Ideally, this test should be run in both directions, to neglect the effect on the wind [Day, 2014]. That was however not a possibility at the test track where the coast down test were performed. After the test, the measurements were used to find the best value of the parameter β to estimate the driving resistance parameters as described in [Rajamani, 2006]:

$$\frac{v_v}{v_{init}} = \frac{1}{\beta}\tan\left[\left(1-\frac{t}{t_{stop}}\right)\tan^{-1}(\beta)\right] \quad . \tag{3.7}$$

Defining the right hand side of Eq. 3.7 as $f(t,\beta)$; for ten equally spaced values of $\beta \in [0.1, 1]$ the one with the smallest value of

$$\varepsilon_\beta = \min_\beta \sum_{n=1}^{N} |\frac{v_v}{v_{init}} - f(t,\beta)| \tag{3.8}$$

was used. With this $\hat{\beta}$; C_d and R_{roll} could be estimated as

$$C_d = \frac{2m_v\hat{\beta}\tan^{-1}(\hat{\beta})}{v_{init}t_{stop}\rho A_f} \tag{3.9}$$

$$R_{roll} = \frac{v_{init}m_v\tan^{-1}(\hat{\beta})}{\hat{\beta}t_{stop}} \quad . \tag{3.10}$$

The slope of the road influences the brake force needed to change the kinetic energy and an estimate of it is used. The available estimated value of the road gradient is an acceleration obtained from accelerometers in the truck. The road inclination at several different locations of the test track is known. Sampling the accelerometer signal φ at some of these location, a linear function from φ to the road inclination could be estimated as the road slope in percent is defined as the value of $\tan(\theta)$:

$$\tan(\theta) = k_\theta\varphi, \tag{3.11}$$

assuming that the slope is proportional to the accelerometer signal with a factor k_θ. The driving resistance from the road slope F_θ may then be implemented in the simulink model as

$$F_\theta = m_v g\sin(\tan^{-1}(k_\theta\varphi)) \tag{3.12}$$

Exponential Cooling

It is assumed that the cooling of the disc is exponential and depends linearly on the vehicle velocity as described in Sec. 3.4. The cooling coefficient b is estimated with the least-squares method. A simplified exponential cooling is implemented in the kinetic energy model, not the convection and radiation model. When the estimations of the cooling coefficients were done, an ambient temperature of 10 °C was assumed. A linear function was fitted to the data points and used for simulations.

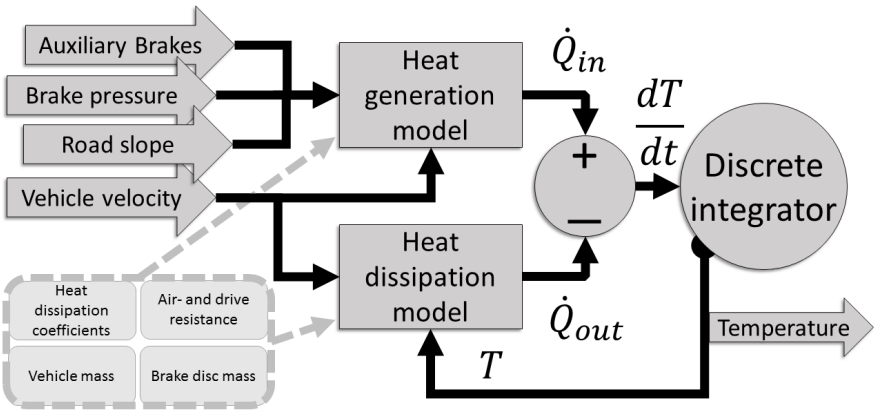

Figure 3.7 An overview of the Simulink temperature model structure (used for all models). The arrows to the left represents the external inputs to the models for heat generation and -dissipation. The difference of the instantaneous heat fluxes is integrated in discrete time and produces the output, the temperature estimate. It is fed back to the heat dissipation model, dependent on current brake temperature and velocity.

3.7 Implementation

Simulink Model

The modeling was done in Simulink, a simulation tool from MathWorks. Two different model approaches were implemented and Fig. 3.7 shows the basic structure. The difference of the heat flux into the brakes and the heat flux out of it is integrated in discrete time, giving the estimated temperature as an output. Based on Eq. 2.2 on p. 7, this structure applies to both of the implemented models (which will be described in the following sections).

Brake Force Model The brake force model use the braking force at the periphery of the wheels together with thermal convection and radiation to estimate the

temperature. The current estimated temperature gives the heat capacity. In total, the thermal convective and radiative heat fluxes are subtracted from the heat generation model. Followed by division of the disc mass and heat capacity a net heat flux is derived as described in Eq. 2.2. Integration in discrete time gives the temperature in each step and thus the temperature is estimated.

Kinetic Energy Model The model based on energy difference does not take into account the absolute value of the brake cylinder pressure. Instead, the difference between the discrete derivative of the kinetic energy and the (discrete derivative of the) work done by the air- and roll resistance forces is used as the heat flux into the disc. This difference is only used as an input when the brake cylinder pressure is nonzero. This may however give rise to the need of other additional inputs; during some of the brake requests from the driver, the auxiliary brakes were used. If this is the case, not all of the lost kinetic energy is heating the brake disc. Some signal processing is needed, like removing the parking brake pressure. The parking brake is only activated while the vehicle is standing still and in this situation no heating of the brakes occurs.

Since the weight per axle is available for the vehicle and the trailer, only the mass of the first axle of the trailer is used in the estimation, due to the fact that the measurements were done at the right wheel on the first axle only. The generated heat is finally divided by two, as there are two wheels per axle. The heat capacity dependency on temperature is implemented as described in Sec. 3.3, with a linear model.

3.8 Brake Pattern Development

To stabilize the vehicle combination in case of jackknifing, the trailer brakes could be pulse braked. This is not intended to slow down the whole combination, just straighten out the vehicle combination. During jackknifing, the trailer is starting to move faster than the truck, and that difference in acceleration should be eliminated by these pulses. To determine this difference, more modeling is needed. One idea is to look at the constant pressure needed for different decelerations, and change the amount of pressure accordingly to get the same amount while pulse braking, see Fig. 3.8 on p. 26.

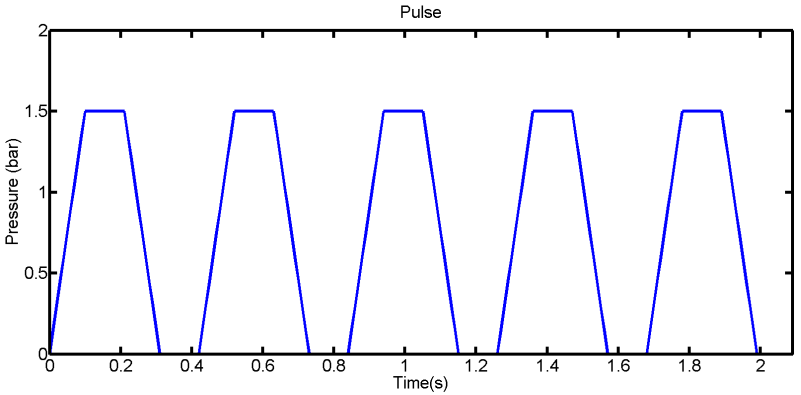

Figure 3.8 The pulse train used for the investigation of the brake pattern influence on the brake disc temperature.

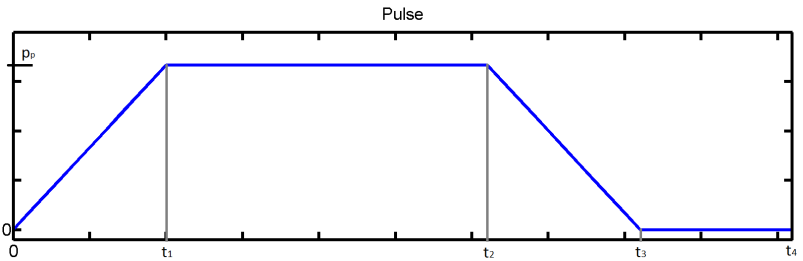

Figure 3.9 Single pulse example.

The brake corridor may be used to determine a suitable pulsed pressure p_p to control the trailer, see Fig. 3.9 for a closer look at one single pulse. The integral of the pulse should be equal to the integral of the constant brake pressure p_c. The following is true assuming that $t_1 = t_3 - t_2$:

$$2 \cdot \int_0^{t_1} \frac{p_p}{t_1} t \, \mathrm{d}t + \int_{t_1}^{t_2} p_p \, \mathrm{d}t = \int_0^{t_4} p_c \, \mathrm{d}t \quad \Rightarrow \tag{3.13}$$

$$p_p \left(t_1 + t_2 - t_1\right) = p_c t_4 \quad \Rightarrow \tag{3.14}$$

$$p_p = p_c \frac{t_4}{t_2} \tag{3.15}$$

Another possibility is to choose a pulsed pressure p_p suitable for all trailers.

4

Results

This chapter presents the results obtained with the different temperature estimation models presented in the method chapter. The results presented include experimental data gathered with a real truck and trailer. First, results used in both the brake force- and kinetic energy model are presented. Furthermore, the result using the different brake force models are presented. Lastly, the kinetic energy model results are presented.

4.1 Truck and Trailer Mass

The axle weight of the truck and trailer for the two different data gatherings are seen in Table 4.1. The measurement was done on a scale suitable for measuring the axle weight on heavy duty vehicles.

Vehicle	Axle	Weight, run 1 (kg)	Weight, run 2 (kg)
Truck	1	7530	7580
Truck	2 + 3	16430	16530
Trailer	1	6860	6770
Trailer	2 + 3	8630	8530

Table 4.1 Axle weights during the two data recordings.

4.2 Heat Capacity

In Sec. 3.3 it was described how the heat capacity for gray iron is modeled. In Fig. 4.1 the result is shown using MATLAB's basic fitting tool. The resulting linear function is:

$$C_p = 0.00045487T + 0.40048. \tag{4.1}$$

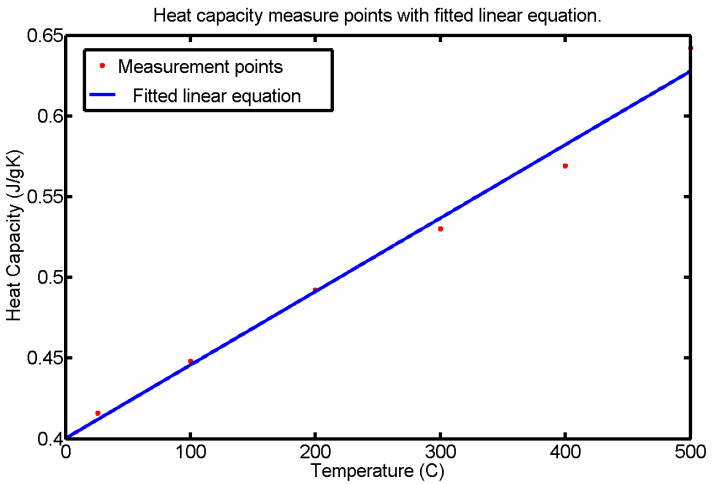

Figure 4.1 The heat capacity as a function of time fitted with data from Fig. 3.5 using MATLAB's basic fitting package.

4.3 Data Sets

The data was acquired on two different occasions. On these occasions several recordings were done. To simplify for the reader the recordings from the first occasion will be called 1:A and 1:B. The recordings from the second opportunity will be called 2:A, 2:B and 2:C.

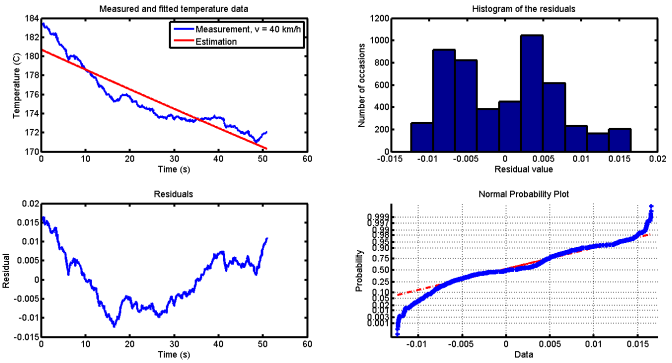

Figure 4.2 Residual analysis for the least-squares estimate of the cooling coefficient while driving with a constant velocity of 40 km/h. The top left figure shows the measured and estimated temperature. The top right figure show the histogram of the residuals, themselves shown in the bottom left figure. The bottom right figure show the MATLAB normplot, see Sec. 4.4.

4.4 Disc Brake Cooling

Fig. 4.2 shows the residuals from the analysis of the cooling coefficient during constant velocity 40 km/h. Fig. 4.3 and 4.4 on p. 30 show the same, but for constant velocity 50 km/h and 59 km/h, respectively. The top left figure shows the measured and the estimated temperature. The top right figure shows the histogram for the residuals, the difference between the measured and the estimated temperature. The bottom left figure shows the residuals and the bottom right figure shows the MATLAB *normplot* in red with the residuals in blue: The closer the residuals, marked in dots, lie to the dash-dotted line, the more the residuals can be described as normally distributed.

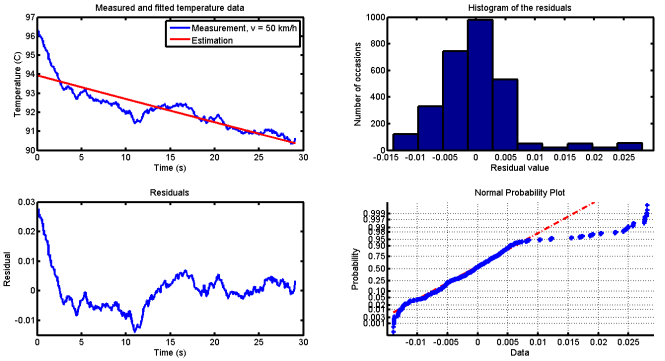

Figure 4.3 Residual analysis for the least-squares estimate of the cooling coefficient while driving with a constant velocity of 50 km/h. The top left figure shows the measured and estimated temperature. The top right figure show the histogram of the residuals, themselves shown in the bottom left figure. The bottom right figure show the MATLAB normplot, see Sec. 4.4.

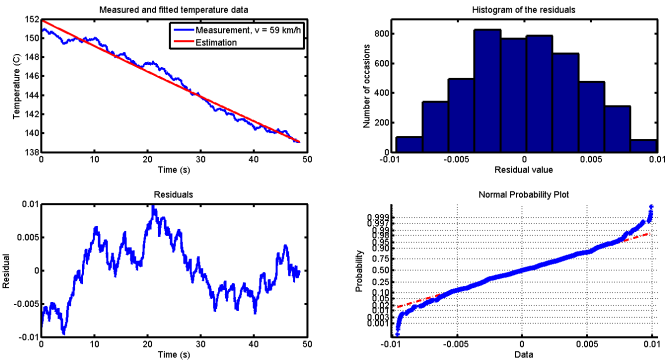

Figure 4.4 Residual analysis for the least-squares estimate of the cooling coefficient while driving with a constant velocity of 59 km/h. The top left figure shows the measured and estimated temperature. The top right figure show the histogram of the residuals, themselves shown in the bottom left figure. The bottom right figure show the MATLAB normplot, see Sec. 4.4.

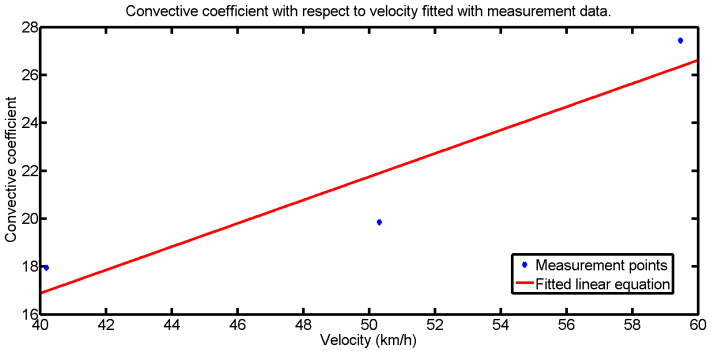

Figure 4.5 The convective cooling coefficient estimation while driving.

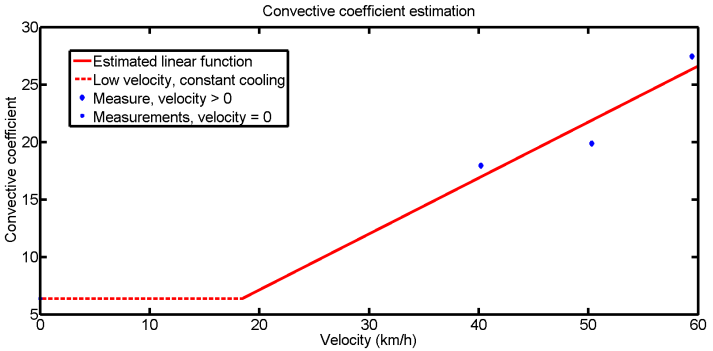

Figure 4.6 The convective cooling coefficient estimation while standing still and driving.

4.5 Brake Force Model

Convective and Radiative Cooling

The convective cooling coefficient was modeled as described in Sec. 3.5. In Fig. 4.5 the convective cooling coefficient while driving is seen. Together with the convective cooling coefficient while standing still, the complete model is seen in Fig. 4.6. Furthermore, the radiative cooling coefficient, $A_s\varepsilon$, was modeled as described in Sec. 3.4, with a value of 0.4.

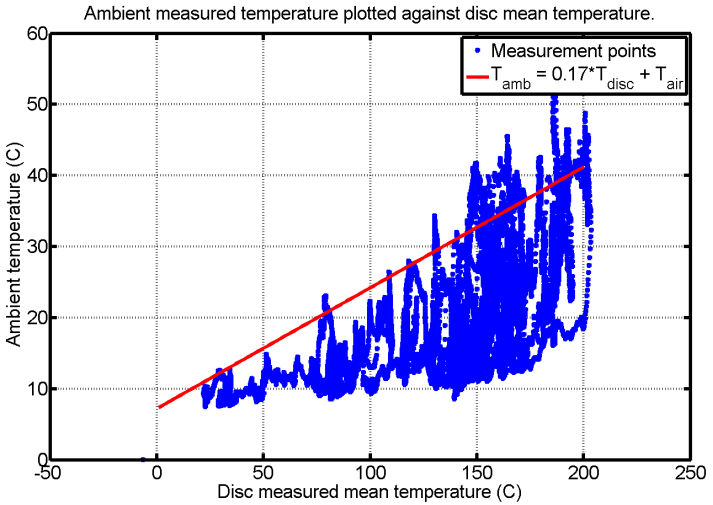

Figure 4.7 The ambient temperature plotted against the disc mean temperature together with a modelled worst case ambient temperature of the disc.

Ambient Temperature of the Disc

The data used to model the ambient temperature of the disc was gathered during the second occasion using the installed thermocouple to measure the surrounding air temperature. In Fig. 4.7 the measurement data together with a worst case linear model of the relationship is seen. The linear function is seen in the legend.

Verification Data Series

Using Table 3.1 with MATLAB's basic fitting tool the control line brake pressure and deceleration relationship is found to be represented by a linear function:

$$a_v = P_m - 0.5 \tag{4.2}$$

which together with the wheel load over the first axle gives the decelerating force:

$$F_w = 3885(P_m - 0.5). \tag{4.3}$$

Together with the thermal cooling this gives the estimation result for the existing data set seen in Fig. 4.8 on p. 33. The first part of the figure shows the estimated temperature together with the measured temperature. Furthermore, the pressure multiplied by a factor 25 is seen. In the second part the absolute error is seen together with the objective threshold.

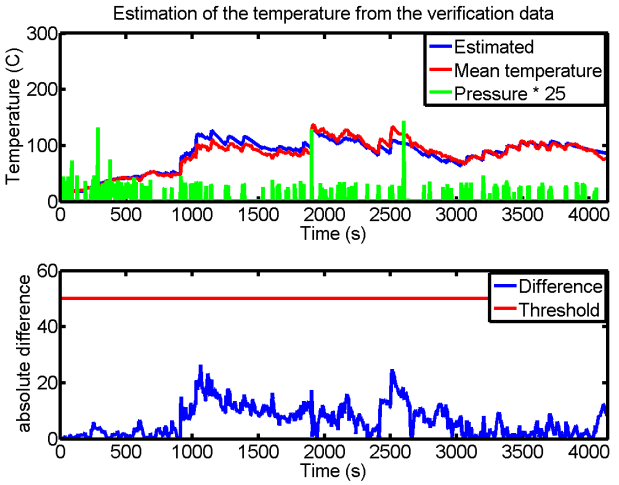

Figure 4.8 Estimation of the temperature for the verification data set.

Brake Corridor

Using the mass of the first axle of the trailer, seen in Table 4.1 on p. 27, an equation describing the worst case decelerating force for a wheel may be derived. This is described in Sec. 3.5. The resulting function is:

$$F_w = 3385 \cdot 9.82 \cdot 0.36 \cdot (P_m - 0.75)/3.8 \tag{4.4}$$

which describes the brake force at the periphery of the wheels of the first axle for the vehicle combination used. The equation only holds for positive brake force values.

Roller Bench Test

The roller bench test was done twice on the first axle, to map the decelerating force to the control line brake pressure P_m. The resulting function describing the relationship was attained through analysis of the result. The gradient of the slope was found to be 4000 N/bar and a brake force was first achieved with a control line brake pressure above 1 bar. The resulting linear function is:

$$F_w = 4000 \cdot (P_m - 1) \tag{4.5}$$

for positive brake force values.

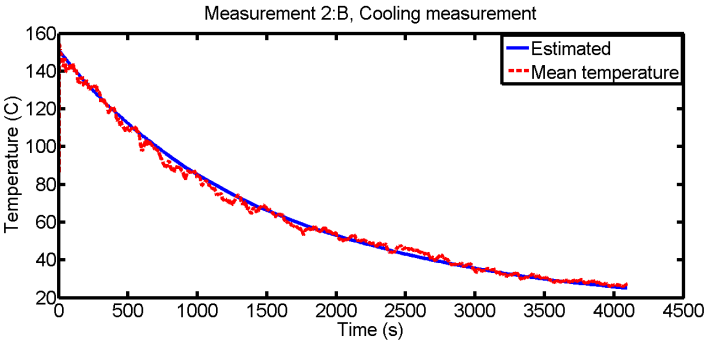

Figure 4.9 Measurement 2:B, the estimated and measured cooling while standing still.

Simulations

Standstill Cooling Using the thermal convection and radiation, the cooling of the trailer brake system was simulated while standing still. This was done using measurement 2:B and the result is seen in Fig. 4.9. Here, the mean measured temperature and the estimated temperature during cooling while standing still is seen.

Brake corridor Measurement 1:A, 1:B and 2:A was used to validate the brake corridor model. The result is presented with two sub-figures. The first sub-figure shows the estimated temperature together with the measured temperature and the control line brake pressure increased by a factor 25. The second sub-figure shows the absolute error together with the objective threshold. In Fig. 4.10 on p. 35 the estimation using measurement 1:A is presented. Furthermore, in Fig. 4.11 on p. 35 the estimation using measurement 1:B is seen. In Fig. 4.12 on p. 36 the result using measurement 2:A is seen.

Roller Bench Test The roller bench test model was used, in the same way as the brake corridor model, to verify the estimation model. For this reason, simulations for the same measurements are presented in the same fashion. For measurement 1:A and 1:B the estimated result is seen in Fig. 4.13 on p. 36 and Fig. 4.14 on p. 37 respectively. The result using measurement 2:A is seen in Fig. 4.15 on p. 37.

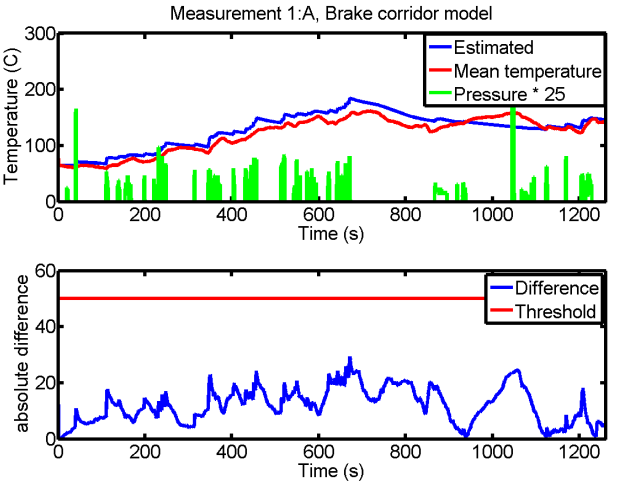

Figure 4.10 Measurement 1:A. The estimation was done using the brake corridor model.

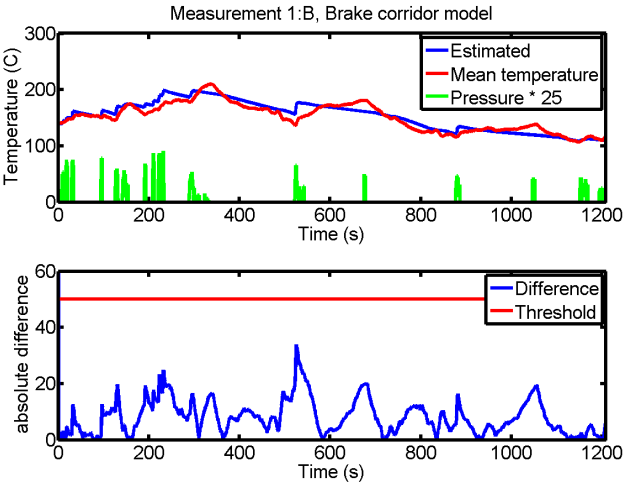

Figure 4.11 Measurement 1:B. The estimation was done using the brake corridor model.

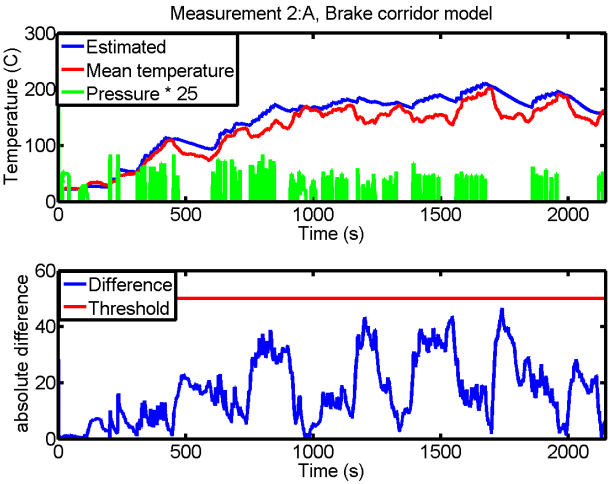

Figure 4.12 Measurement 2:A. The estimation was done using the brake corridor model.

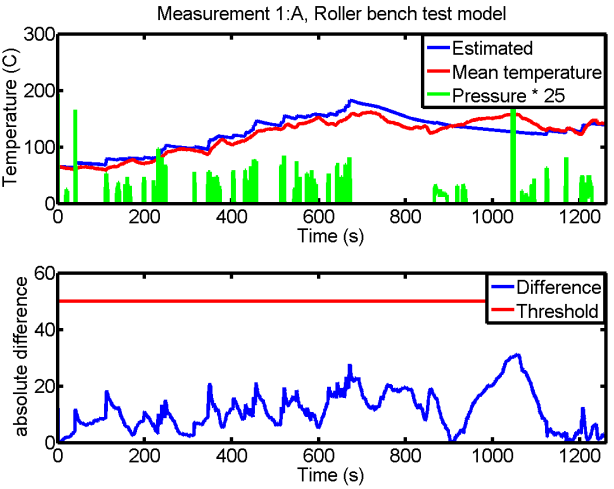

Figure 4.13 Measurement 1:A. The estimation was done using the roller bench test model.

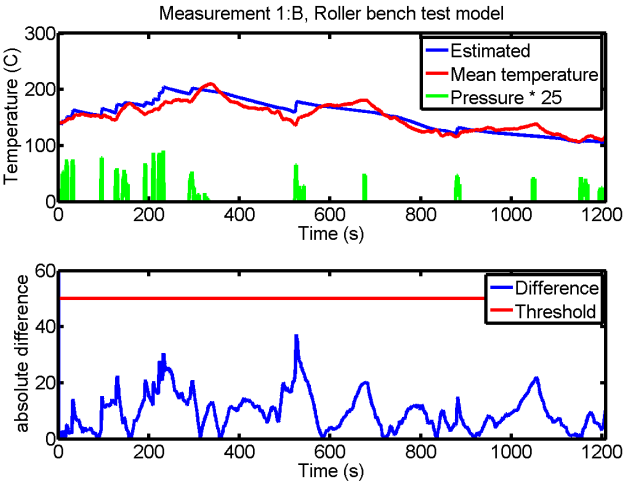

Figure 4.14 Measurement 1:B. The estimation was done using the roller bench test model.

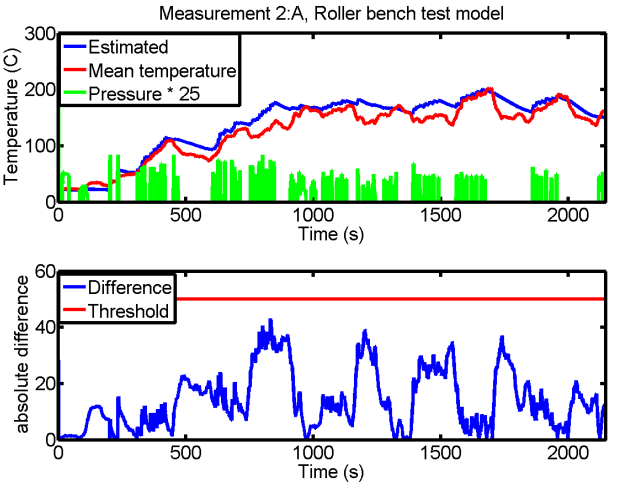

Figure 4.15 Measurement 2:A. The estimation was done using the roller bench test model.

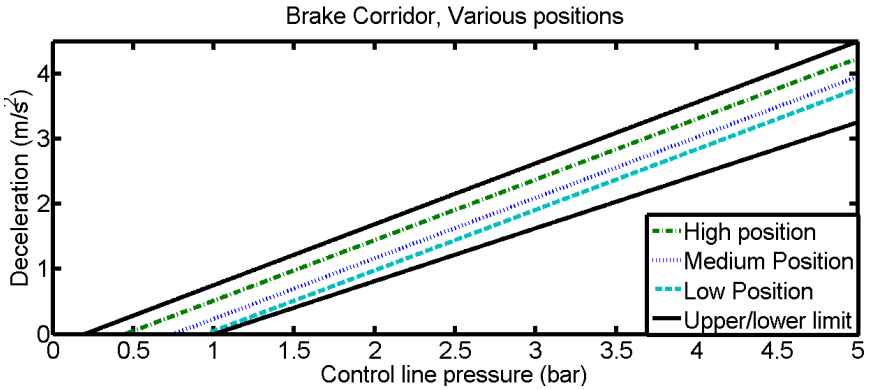

Figure 4.16 Various brake corridor positions.

Brake corridor analysis

To investigate how the model behaves if the brake corridor model is wrong, two new brake corridor positions were constructed. One higher and one lower than the one used in the simulations, see Fig. 4.16. The higher one is:

$$F_w = 3385 \cdot 9.82 \cdot 0.36 \cdot (P_m - 0.45)/3.8 \tag{4.6}$$

and the lower one is:

$$F_w = 3385 \cdot 9.82 \cdot 0.36 \cdot (P_m - 0.95)/3.8 \quad . \tag{4.7}$$

Together with the high and the low brake corridor positions the temperature was estimated for measurement 2:A. The result is seen in Fig. 4.17 on p. 39. The estimated temperatures together with the measured temperature is seen in the first sub-figure. In the second sub-figure the absolute error is seen together with the objective threshold.

Furthermore, the brake corridor model was compared with the roller bench test model for the measurement setup used. The result is best visualized as deceleration in the brake corridor and the result can be seen in Fig. 4.18 on p. 39.

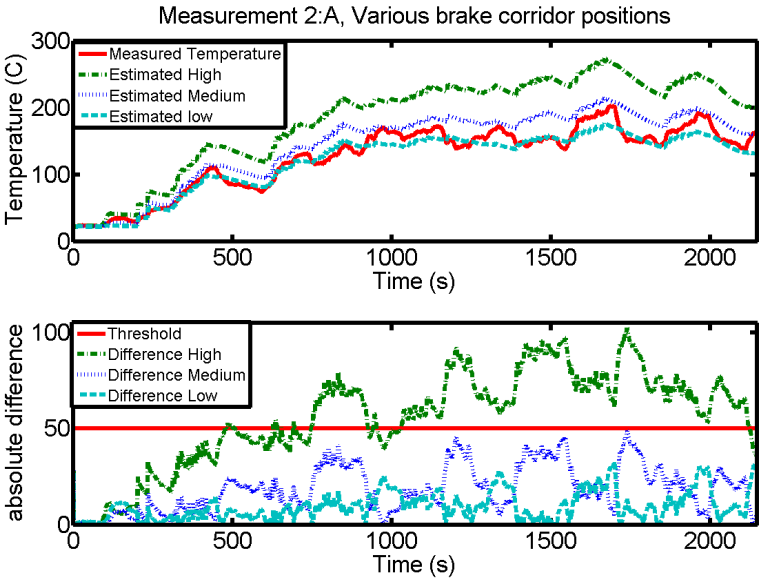

Figure 4.17 Temperature estimation result for measurement 2:A.

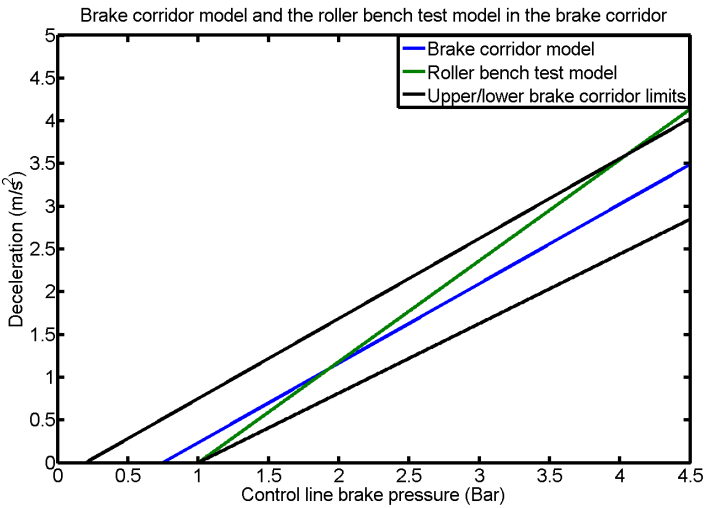

Figure 4.18 The position of the brake corridor model and the roller bench test model in the brake corridor.

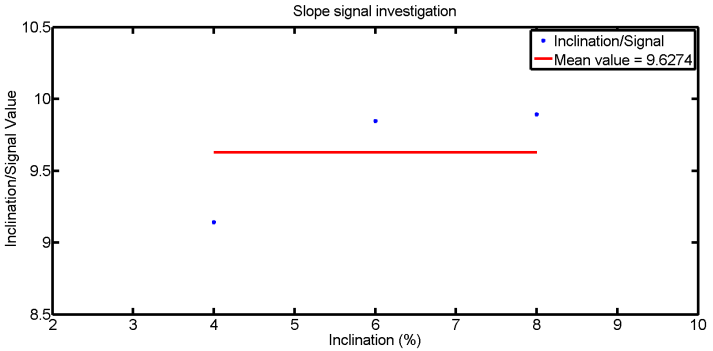

Figure 4.19 The investigation of the acceleration signal to known inclinations on the Scania Test Track. The ratio of the the known road gradient and the signal φ is marked by dots and the line marks the mean value, used in the model.

4.6 Kinetic Energy Model

See Table 4.2 for the estimated parameters for the different coast down-tests: the air resistance coefficient and the roll resistance (per axle). In the case when two estimations of the driving resistance coefficients were done, during the same data recording, the mean value between the estimations is used in the simulations.

Experiment	Initial velocity (km/h)	C_d	R_{roll}/axle	ε_β
1:A	21.6	4.1296	322.5015	156.8917
1:B	30.2	3.0082	352.8864	95.9271
1:B	40	0.5320	435.8862	138.0276
2:C	27.7	3.8502	64.4856	106.4455
2:C	41	1.3653	386.9135	181.2826

Table 4.2 Estimated air- and roll resistance from measurement data.

See Fig. 4.19 for the investigation of the factor k_θ, used in Eq. 3.11 on p. 23. The parameter $\hat{k_\theta}$ was chosen as the mean value of the three observations, obtained as the ratio between the known slope and the measured accelerometer-based signal.

Fig. 4.20 on p. 41 shows the result from the cooling coefficient estimation, based on measurements during stand still and driving with constant velocities. The figure also shows the bilinear curve, used for simulations, in red. The linear curve is fitted to the four data points and limited to the cooling level at stand still.

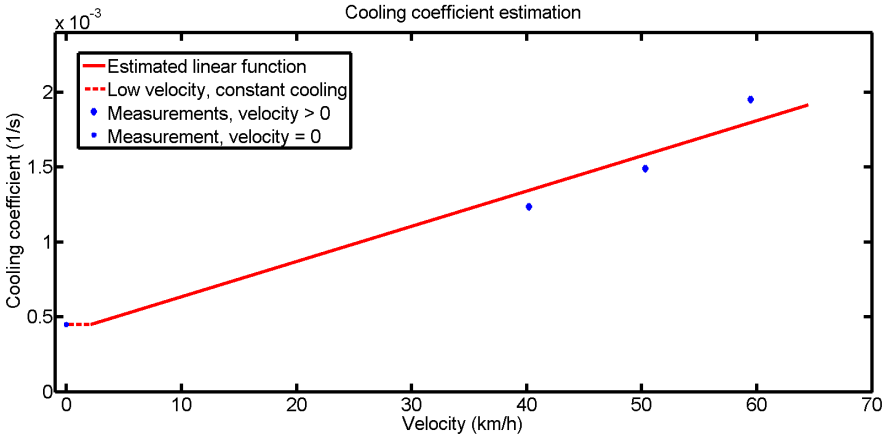

Figure 4.20 Least-square values of the cooling coefficients for different velocities. A linear function is fitted to the four data points and limited to the value at zero velocity.

See Fig. 4.21 on p. 42 for the simulated temperature compared to the measured temperature during cooling when the truck was standing still (measurement 2:B). The least-squares estimate of the cooling coefficient is $b = 4.5 \cdot 10^{-4}$.

Several simulations were done based on the collected data. The first sub-figure shows the simulated temperature, compared to the mean temperature between the inner- and the outer thermocouple measurement. The brake pressure (in bar) is magnified 25 times to show the locations in time of the energy input to the model. The second sub-figure shows the absolute value of the difference between the estimated and the measured mean temperature and the 50 °C threshold. Fig. 4.22 on p. 42 shows the result from measurement 1:A. The simulation was done both with and without the road gradient implementation and both is presented in the figure. The same evaluation is done in Fig. 4.23 on p. 43 showing the result from measurement 1:B. Fig. 4.24 on p. 43 shows the results from measurement 2:A.

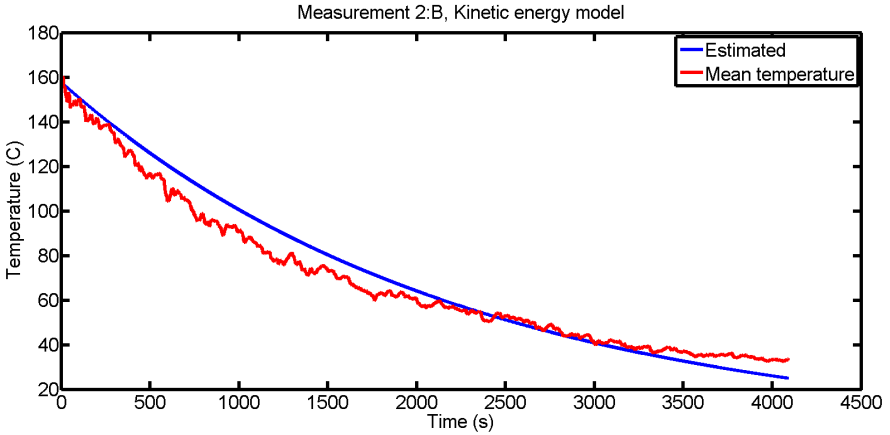

Figure 4.21 Measured and estimated temperature of the disc brake while the truck is parked, measurement 2:B.

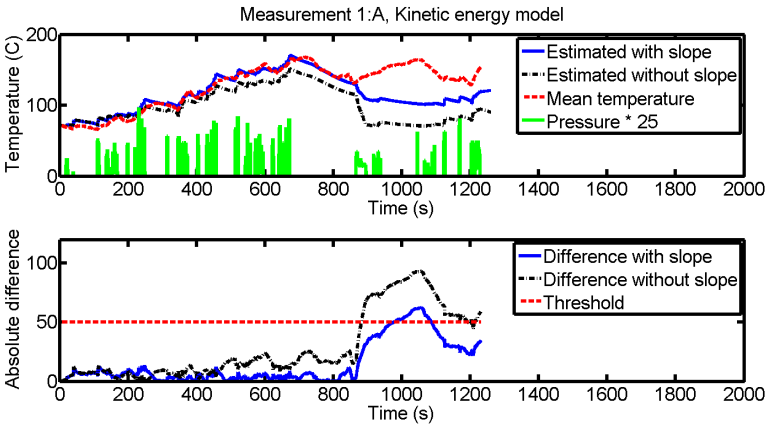

Figure 4.22 Simulation of measurement 1:A at the test track at Scania. This figure also shows the temperature estimation without the road slope implementation.

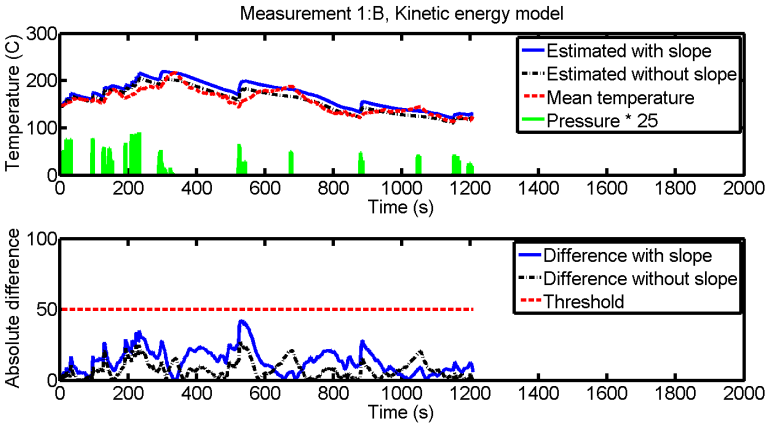

Figure 4.23 Measurement 1:B at the test track at Scania. This figure also shows the temperature estimation without the road slope implementation.

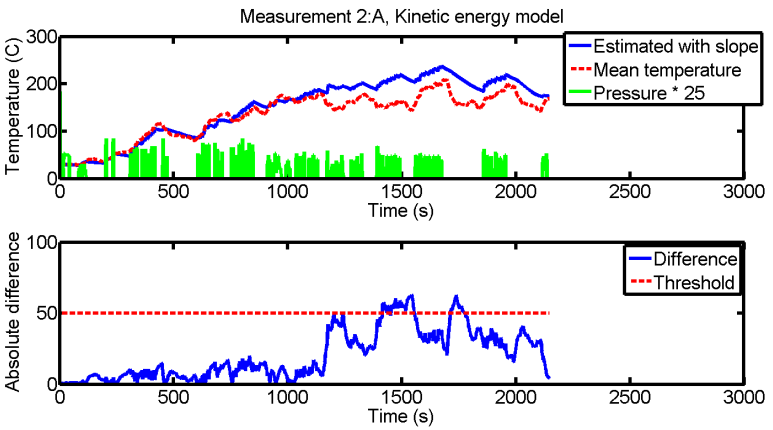

Figure 4.24 Measurement 2:A at the test track at Scania.

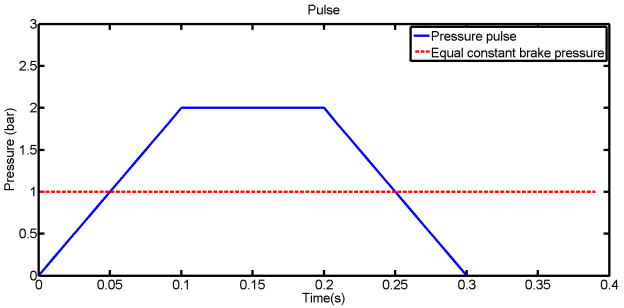

Figure 4.25 Pulse used for investigation of temperature obtained in the brake during safety braking. Here with a pulsed pressure p_p of 2 bar.

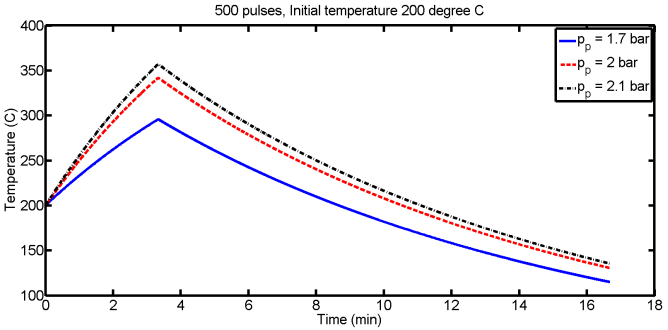

Figure 4.26 Simulated temperature with pulsed braking using different pressures. Initial temperature is 200 °C and 500 pulses is actuated. Parameter values are the same as in Table 4.4.

4.7 Brake Pattern Development

One pulse used for investigation may be seen in Fig. 4.25. The pulse pressure p_p equals a constant pressure of $p_c = 0.5p_p$. The results can be seen in Table 4.3 on p. 45 showing the pulse pressure, the pulse length, the initial temperature, the number of pulses and the temperature increase. Values used in the simulation may be seen i Table 4.4 on p. 45. The brake corridor position refer to the positions in Fig. 4.16 on p. 38. In Fig. 4.26 a plot showing the cooling behavior can be seen. An investigation of the sensitivity to inaccurate parameter estimations may be seen i Table 4.5 on p. 45. These results were simulated with the brake corridor model. Because of mechanical restrictions, brake pulses can at most be actuated 2-3 times per second.

p_p	t_4	N	Init. temp. (°C)	End temp. (°C)	Temp. increase (°C)
1.7	0.4	500	150	263	113
1.7	0.4	500	200	296	96
1.7	0.4	500	300	360	60
1.7	0.4	10 000	all	456	-
2	0.4	250	150	240	90
2	0.4	500	150	311	161
2	0.4	250	200	280	80
2	0.4	500	200	342	142
2	0.4	250	300	358	58
2	0.4	500	300	403	103
2	0.4	10 000	all	539	-
2.1	0.4	500	150	327	177
2.1	0.4	500	200	357	157
2.1	0.4	500	300	417	117
2.1	0.4	10 000	all	563	-

Table 4.3 Investigation of temperature from pulsed braking (2.5 Hz). Time between initial and end temperature is 200 s for 500 pulses.

Parameter	Value
Axle mass	6770 kg
Velocity	40 km/h
Brake corridor position	medium

Table 4.4 Parameters used for the brake temperature simulation. See Fig. 4.16 for the brake corridor positions.

Parameter	Deviation	End temp. (°C)	Temp. rise (Δ °C)
Axle mass	+50%	422	+56%
Axle mass	+20%	375	+23%
Axle mass	-20%	308	-24%
Axle mass	-50%	254	-61%
Total cooling	+20%	331	-7%
Total cooling	-20%	354	+8%

Table 4.5 Investigation of sensitivity to parameter deviation, p_p = 2 bar. Parameter values as in 4.4. The input signal was 500 brake pulses and the initial temperature was 200 °C. The temperature rise column state the ratio between the new estimated temperature increase and the old temperature increase (without parameter change).

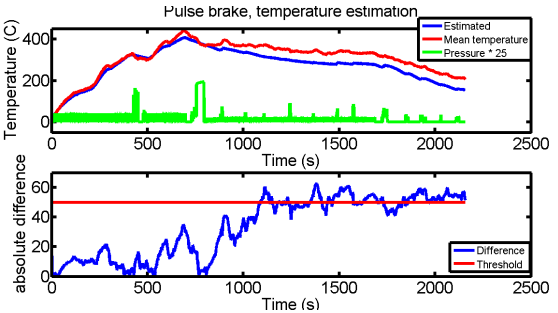

Figure 4.27 Temperature measurement at the first axle (right wheel) while pulse braking with two different control line pressures. At first with $P_m = 1.7$ and then, after around 800 s with $P_m = 0.8$.

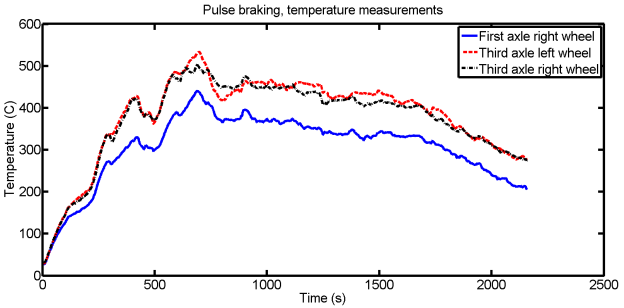

Figure 4.28 Temperature measurement at three wheels while pulse braking, illustrating the temperature difference between the first and the third axle.

Using new thermocouples on the same trailer as before, a measurement using an implemented pulse brake function was conducted. For this simulation a new brake corridor position was used:

$$F_w = 3385 \cdot 9.82 \cdot 0.36 \cdot (P_m - 0.47)/3.8. \tag{4.8}$$

The result can be seen in Fig. 4.27. The figure shows the estimated temperature, compared to the measurement from the right wheel on the first axle, while pulse braking. First with a control line brake pressure of 1.7 bar and then, after around 800 s, with a control line brake pressure of 0.8 bar. The temperature for the third axle (both wheels) was also measured and the result can be seen in Fig. 4.28.

5

Discussion

In this chapter the results from the previous chapter are discussed and assessed. The focus will be on the modeling approach, the different models and the equipment.

5.1 Modeling Approach

With a lumped capacitance model, the bulk temperature, not the surface temperature, is estimated. Since the models assume that the temperature in the disc is uniform, the estimation is validated against the mean temperature between the inner and the outer temperature measurement. It can then be assumed that the more thermocouples used, the better the mean temperature of the disc is measured.

It is noticed that some of the peaks in the measured mean temperature do not align with the estimated temperature peaks. This may depend on the simplified modeling of the bulk temperature as a uniform temperature. Hence, the heat generation into the disc is assumed to spread throughout the disc instantaneously. In reality this is not the case, as seen in the measurements, especially in Fig. 4.11 on p. 35.

5.2 Equipment and Data Analysis

Data Gathering

Temperatures over 300 °C were hard to acquire in the disc brake with the casual driving regime used. Cooling data at constant velocities were also hard to get, as the test track is not flat.

Thermocouple Analysis

It was seen, before the second data gathering, that there was an offset between the two thermocouples before any heating of the disc was done. To fix this, the offset was removed after the data was gathered. The thermocouples were tested after

they had been dissembled from the trailer and the offset could be noted. The offset increased as the temperature increased, indicating that one of the thermocouples was measuring the wrong temperature. When new thermocouples was used, the position in the brake corridor was updated according to new experimental data. However, the cooling model was not updated as no new cooling data was acquired.

Data Analysis

During some of the measurements, unexplained increases of the temperature was noticed. This may be seen in Fig. 4.11 on p. 35 around the 1000 second mark. Note that no braking had occurred for a decent amount of time, but still the temperature is increasing in the disc. This behavior occurs in several measurements but the reason is unknown. However, what is known is that it is a result caused by driving the vehicle combination. The behavior was not seen while standing still.

5.3 Ambient Temperature of the Disc

During the data acquisition of the ambient temperature around the disc brake, it was noticed (and shown in Fig. 4.7 on p. 32) that the measured temperature was fluctuating a lot. The temperature fluctuations does not depend only on the vehicle velocity. This, since the fluctuations occurred equally much on lower as on higher velocities. The fluctuations also occurred while standing still.

The measured result that was expected was a measured ambient disc brake temperature that grew until a steady state temperature was achieved. This was not the case. This is why a linear function was fitted to the top temperatures of the measurements to represent a worst case scenario. Why the measured ambient temperature of the disc brake was fluctuating was not investigated further.

5.4 Cooling Coefficient Estimation

Cooling data when driving with constant velocity is only available for short periods of time (around 60 s). This because the test track used to gather the data did not provide sufficient long distance without any inclination. More data on the cooling behavior is desirable. An analysis of the validity of the least-squares estimations may be seen in Figs. 4.3 and 4.4 on p. 30. The residuals does not look perfectly normally distributed. Especially in the beginning, the residuals are considerably bigger than during the rest of the time span. The data was obtained during two different occasions. Weather conditions were not measured. Wind and outside temperature influence the cooling behavior and generality cannot be ensured. Too little data was collected and no conclusions should be based solely on it.

As indicated above, the cooling of the disc seems to depend on a lot of different parameters. This makes it hard to derive a model that takes into account the randomness of driving in different weather conditions. It is however seen that the simplification, that the cooling coefficient depends linearly on the vehicle velocity, is good.

5.5 Brake Force Model

Convective and Radiative Cooling

The convective coefficient was determined from the cooling coefficient using Eq. 3.2 on p. 20. For simplicity, the heat capacity was assumed to be constant during the cooling as described in Sec. 3.4. This simplification works well, mainly because the temperature range is low. Hence, the change in heat capacity is not big, see Fig. 4.1 on p. 28. If the valid temperature range is increased, there is a possibility that the change in heat capacity is too big and affects the result, resulting in a bad convective coefficient estimation. Including a heat capacity with temperature dependency in turn gives a more complex model since Eq. 2.21 is not adequately solved by Eq. 2.22 on p. 14. However, the simplification is working well during this work.

The radiative coefficient is complex to model. This due to the disc area subject to radiation needs to be known as well as the emissivity. In Sec. 3.4, it is mentioned how the emissivity changes depending on the level of oxidation of the disc surface. This, and the fact that the radiation is such a small contribution with respect to convective cooling, led to the decision to use the radiative coefficient as a design parameter. The value is reasonable.

A measurement while standing still was performed and the result is shown in Fig. 4.9 on p. 34. The estimation represents the measurement very well. In fact, the result is better than only using the exponential cooling seen in Fig. 4.21 on p. 42. A conclusion being that a cooling model using both convection and radiation is working very well.

Verification Data Set

The model estimates the temperature with an accuracy of 25 °C, see Fig. 4.8 on p. 33. Since the objective is to have an accuracy of $\pm$ 50 °C, the estimation is satisfying the objective.

An advantage with this data is that it is gathered during a normal drive in and around Södertälje for a long duration of time, representative for a typical driving scenario. It can be seen from this data that the control line brake pressure is normally between 1 to 2.5 bar. When exceeding this, the braking situation is not considered pleasant for the driver.

Brake Corridor

In Figs. 4.10 to 4.12 on p. 35 to 36 the result from the brake corridor model is seen. The estimation is performing well and is within the 50 °C threshold. In Fig. 4.12 on p. 36, the result during measurement 2:A is seen. During this simulation, the accuracy is worse than in Figs. 4.10 to 4.11. It can be seen around the 1200, 1500 and 1750 second mark that the measured temperature is decreasing much faster than the estimated temperature. The reason behind this behavior is unknown, seen in the other simulations with the other models, and more testing needs to be done to determine the origin of the problem. However, the estimated temperature is within the objective accuracy and satisfies the goal.

The aim with the brake corridor model was to find a general case position working for various trailer and truck combinations. Since all trailers are different, this is challenging. In Fig. 4.17 on p. 39, different positions in the brake corridor was used to estimate the temperature. This was done to see how different positions in the brake corridor affects the estimation. It is seen that a higher position with a conversion parameter value x of 0.45 bar (60 % of the conversion parameter value used in the medium position) results in an error up to 100 °C. The objective accuracy is not fulfilled and is thus not acceptable. The lower position in the brake corridor with a conversion parameter value of 0.95 bar (127 % of the conversion parameter value used in the medium position) gives less error, even less error than the medium position used in the normal simulations. However, it is seen that the result using the lower position in the brake corridor underestimates the temperature.

The mass load over each axle on the trailer has to be known in the brake corridor model. During the project, it is assumed that these masses are known. However, this is not true for every trailer. This problem is not taken into account in this master's thesis.

Roller Bench Test

The roller bench test was done to find the characteristics of the trailer brakes. It is seen in the result in Sec. 4.5 that the trailer uses a very low brake cylinder pressure with respect to the control line brake pressure. This is because the trailer is loaded lightly; the brakes in the trailer is therefore activated at the lower boundary of the brake corridor. However, the gradient of the linear slope is still very high. This could be because the trailer brake system is fairly new.

The achieved result with the roller bench test model is seen in Figs. 4.13 to 4.15 on p. 36 to 37. The result is very similar to the result of the brake corridor model. The slope achieved with the roller bench test is very high compared to the brake corridor model. Even the conversion parameter, x, between the models is different. This is very interesting since the initial guess was that these heat generation models should be roughly the same. Thus, either one of the models could be questioned

whether it is true or not. What is known is that some trailer's electronic system can recognize that it is doing a roller bench test. If so, the trailer will brake as if it were fully loaded even though it is not. Hence, the result from the roller bench test can give a bad result, not describing reality. This can also be the reason why the roller bench test model leaves the brake corridor around a control line brake pressure of 4 Bar. To verify this, a roll out test, see Sec. 3.2, could be done. The roll out test should give the exact deceleration for the current vehicle combination and thus also for the trailer. However, since the brake corridor model is the model of highest interest, this was not done.

The difference between the brake force models is big and it is interesting to know why they are giving similar results. The reason is that the difference in the calculated brake force between them both, for low control line brake pressures (around 2 bar), is not too big, see Fig. 4.18 on p. 39. Furthermore, it can be motivated that if higher control line brake pressures are used, the models will deviate a lot from each other. The conclusion should, however, not be that every brake corridor position gives roughly the same calculated brake force for low control line brake pressures. This was shown in Fig. 4.17 on p. 39.

The negative aspect of using the roller bench test model in the future implementation is that the test needs to be redone and implemented for each new load distribution. This would probably be too inconvenient for the driver and the function would therefore not be used.

5.6 Kinetic Energy Model

The estimation of the measured temperature on the trailer's brake disc is satisfying under the conditions during the data recordings. However, if this temperature model is to be used, the following is problematic; Initial knowledge and inputs to the model are presumed or needed:

- Vehicle weight,
- number of wheels,
- air resistance coefficient C_d,
- roll resistance R_{roll},
- road gradient and
- if auxiliary brakes are in use.

Especially the driving resistance parameters differ a lot between executive tries. Estimations of the weight and knowledge about the number of wheels are available on the truck through its electric system, but not necessarily about the trailer. The accelerometer used for this thesis is not available in commercial trucks. Other road gradient estimations are available with varying accuracy. But, as can be seen in Fig. 4.22 on p. 42, the road gradient does not account for a big difference in the result. The difference between the estimation and the measurement still lie below the threshold. Another measurement from the same occasion, seen in Fig. 4.23 on p. 43, becomes better *without* the implemented road slope influence. The two measurements uses different estimations of driving resistance parameters C_d and R_{roll}, see Table 4.2 on p. 40, and the contrarious results probably originate from these estimations.

Fig. 4.22 highlights another problem following the kinetic energy model: At 900 seconds, this model cannot capture the driver's behavior, using the accelerator and the brake pedal almost instantaneously. The brakes are heated, but no temperature increase is seen in the simulation.

In Fig. 4.24 on p. 43, showing the simulation from measurement 2:A, the difference is bigger than the desired threshold at several occasions. It does not look like the difference between the simulation and the measurement is growing, instead it decreases back to desired levels every time. A source for these fluctuations is yet to be suggested.

The influence of the auxiliary brakes is not implemented in this model. During normal driving, these are typically used instead of (or in combination with) the service brakes to retard the vehicle. Therefore, they must be taken into consideration if this model is used to predict the temperature in the brake disc.

Driving Resistance The estimated parameters in Table 4.2 does not give a consistent picture regarding the roll- and air resistance influencing the vehicle combination on the test track. Ideally, these parameters should be estimated anew each time this model should be used which is not practical nor generally useful. The best (smallest value of the total deviation in the last column of Table 4.2) estimation of the air resistance does not lie close to the real value: 0.5-0.6 (depending on the vehicle configuration). More data, especially with higher initial velocities, would be interesting. The Scania test track does not allow for this as the straight non-hilly part of the track is too short.

Brake Disc Cooling The ambient temperature and the radiation is not implemented in this model and the result is clearly not as good as with the more complex model. The assumption, that the cooling of the disc is solely exponential, gives reasonably good results.

5.7 Comparison of Results to Other Work

The results presented in this thesis compares good to other work on temperature estimation in disc brakes. Earlier work on temperature modeling using the lumped capacitance model present errors exceeding 50 °C [Nisonger et al., 2011]. However, this is over a bigger range of temperatures in the brake disc than presented in this work and a more aggressive braking pattern is used. In [Sheridan et al., 1988], generally similar model approaches gives similar results (maximum errors around 50 °C).

Estimations done with other methods, like computational flow dynamics (CFD), give errors in the same range as the lumped capacitance model. This modeling approach is however not suitable for implementation in trucks, rather for disc development.

5.8 Brake Pattern Development

The model based on the brake corridor was used for the investigation of brake patterns. Mainly because of the possibility to use an arbitrary pressure curve as an input. A simulated constant velocity of 40 km/h is reasonable, as a preliminary requirement for the safety function to be active is a velocity below 50 km/h.

As can be seen in Fig. 4.26 on p. 44, the cooling of the brakes is a slow process. The temperature rise created by the pulsed braking must not be so high that the service brakes cannot be used. One extreme situation is the ”alpine descent”, when driving at a constant speed (maintained by braking) downhill for a long time. (The recommendation for such situations is, however, to use the auxiliary brakes like the retarder or exhaust brake instead of the service brakes). If jackknifing would occur during such circumstances, the brakes could already be too hot when the safety hazard is detected. In the case of fading, these low pressure brake pulses would not be enough to avert the dangerous situation.

The pulsed braking was simulated during several minutes, which is an unlikely incidence during normal driving. Smaller temperature rises can be expected during intended interventions. It should be remembered that the estimated temperature is the bulk temperature of the disc and little can be said about the surface temperature, or the temperature distribution inside the disc.

Pulse Brake Function

Together with a new brake corridor position, the pulse brake function was tested on Scanias test course, see Fig. 4.27 on p. 46. A new, higher, brake corridor position was used according to the measurements from the new thermocouples. What can be seen is that the temperature estimation model works well for higher temperatures.

Though, with the pulsed control line brake pressure of 0.8 bar, the absolute difference increases to around 50 °C. This is at the boundary of what is acceptable. It is possible that more modelling is needed for very low pulsed brake pressures. For example, dragging brake pads or other mechanical effects could be a reason for the difference in temperature.

Using the new thermocouples, the temperature in three of the trailer's brakes was measured. It can be seen in Fig. 4.28 on p. 46 that the brakes on the third axle is hotter than the brake on the first axle is. One reason could be that this axle brakes more aggressively than the first axle. Another possible reason is that the aerodynamics around the disc is worse than around the wheel on the first axle, as it is placed immediately behind the second axle. The combination results in higher temperatures, which needs to be considered in a future implementation of the pulse brake function.

6

Conclusion

This chapter summarises and gives the concluding thoughts of the work that has been performed in this master's thesis.

All models perform sufficiently good. However, the brake force model is more suitable than the kinetic energy model to implement in a truck, as the driving resistance parameters and the auxiliary brakes does not influence the temperature estimation. The brake force model uses the control line brake pressure, the velocity and the measured air temperature as inputs to return the temperature as the output. Within the brake force model there are various heat generation models. The most general one is the brake corridor model. The exact placement of a single trailer inside the brake corridor is unknown but regulated by [*Vehicle Regulations UN ECE-R13* 2008]. Therefore, the generated heat in a worst case scenario for a particular control line brake pressure should, by law, be within the lower and upper limit of the brake corridor curve.

The other brake force heat generation models can also be used to estimate the temperature. They are performing equally good as the brake corridor model. However, the consequence of using them are that the brake characteristics change with time and experiments have to be done to update the model. To use the brake corridor heat generation model, only the trailer load over each axle must be known.

The brake pattern study suggests that the steady state temperatures lie below critical temperatures, which allows further development of the jackknife safety function. More analysis is needed to determine which parameters are most important for the temperature rise in the disc. Late experimental data indicates a higher brake corridor position. That results in higher steady state-temperatures than in the simulations in Sec. 4.7.

7

Future Work

As of now, the temperature estimation model is not ready to be implemented in a truck for estimation of the temperature together with a random trailer. However, the result is promising. In this chapter, suggestions are made for the continuation of the work done in this master's thesis. The focus will be on making the temperature estimation model ready for use. This includes further investigation of the cooling characteristics, better knowledge about higher temperatures and an investigation of the brake corridor model with the aim to make it as general as possible.

7.1 Cooling Data

It has been mentioned in the report that the cooling data is not sufficient. It would be advisable to further investigate the cooling in the temperature estimation model. Therefore, it would be needed to gather better cooling data for various velocities and under a substantial duration of time. It could also be done in a more controlled manner in a test rig. Such a test rig exists on Scania, but was not available for usage during the master's thesis. This test rig uses the disc brake system together with a controllable air fan and can be used to simulate driving at various constant velocities.

To improve the measurement, drilled-in thermocouples could be used. This would allow for better temperature measurement, less influenced by the complex air flow around the disc. However, the brake disc and pads need to be switched out after the measurements, which is why this was not done.

7.2 Modelling Low Brake Pressures

During the last run on the test track, effects concerning low threshold brake pressures was visible. The model did not fully capture the heat generation, seen in the latter part of Fig. 4.27 on p. 46, when the control line brake pressure was small.

7.3 Extensive Model Validation

Various Driving Courses

The temperature estimation model has to be checked for various driving scenarios. The alpine descent test is recommended since it is one of the cases where the stabilizing function could be activated. Scania's test course is not sufficient for this purpose since it has many turns and hilly terrain. Also, casual test driving around Södertälje using the brakes both passive and aggressive during different weather conditions could further verify the temperature estimation model.

7.4 Expanding the Temperature Estimation Model

Drum Brakes

During this project only disc brakes were discussed. However, the drum brake system is also common and thus, expanding the model to include the drum brake system is desirable. To include drum brakes it must be investigated how well the modeling approach, assuming uniform temperature, fits with the brake system. Furthermore, cooling data and cooling coefficients needs to be derived. If the modeling approach holds, the same methods used to investigate the disc brake system can be used. It is likely that drum brakes have worse cooling characteristics than disc brakes, since the heated surface is inside the drum instead of in contact with the air, flowing around the wheel. If the drum brake system is heated to a high temperature faster than the disc brake system, it must be investigated how well the stabilizing brake function would work with the drum brake system.

Different Trailers

The aim of the temperature estimation model is to make it work for various trailers. For this purpose, different trailers have to be investigated in order to verify that the assumption that most trailers are located in the lower part of the brake corridor, is true. Furthermore, a statistical analysis of the accuracy achieved with different brake corridor positions, in order to determine the best brake corridor position, has to be done.

7.5 Influence of Auxiliary Brakes

If the kinetic energy model is to be used in a vehicle, the auxiliary brakes must be taken into account. The experimental data was mostly obtained with these brakes deactivated. During normal driving, they are used to unburden the friction brakes and the energy does not heat the service brakes. In the trucks electric system, information regarding the torque from the auxiliary brakes are readily available to be fed to the model.

Bibliography

10-00 Bromskunskap (2015). Scania CV AB. Scania Research and Development, 151 87 Södertälje, Sweden.

Alonso, M. and E. J. Finn (1980). *Fundamental university physics*. 2nd ed. Addison-Wesley Publishing Company, Inc., USA.

Bejan, A., ed. (1993). *HEAT TRANSFER*. John Wiley & Sons, Inc., 5353 Dundas Street West Suite 400 Toronto, Ontario M9B 6H8 Canada.

Day, A. J., ed. (2014). *Braking of Road Vehicles*. Butterworth-Heinemann, 30 Corporate Drive Suite 400, Burlington MA 01803, UK.

Day, A. J., J. Klaps, and C. F. Ross, eds. (2012). *Braking of Road Vehicles*. Inprint and Design Ltd, University of Bradford, Bradford, BD7 1DP, UK.

Fransson, C. (2009). *Pressure to torque gain estimations for pneumatic disc brakes with use of slip and friction based methods in heavy duty trucks*. ISRN: LIU-IEI-TEK-A–09/00590–SE. MA thesis. Linköpings universitet TEKNISKA HÖGSKOLAN, SE-581 83 Linköping, Sweden.

Hammarström, U., R. Karlsson, H. Sörensen, and M.-R. Yahya (2012). "Coast-down measurement with 60-tonne truck and trailer. estimation of transmission, rolling and air resistance." *Statens väg- och transportforskningsinstitut*. Dnr 2008/0543-24.

Hwang, P., X. Wu, and Y. Jeon (2008). "Repeated brake temperature analysis of ventilated brake disc on the downhill road". *SAE Technical Paper 2008012571*.

Ihm, M. "Introduction to gray cast iron brake rotor metallurgy". In: TRW Automotive. SAE tutorial.

Johansson, R. (2012). *System Modeling & Identification*. Prentice Hall, Prentice Hall, Englewood Cliffs, NJ.

Kwangjin, L. (1999). "Numerical predicition of brake fluid temperature rise during braking and heat soaking". *SAE Technical Paper 1999010483*.

Lienhard IV, J. H. and J. H. Lienhard V (2011). *A Heat Transfer Textbook*. 4th ed. Phlogiston Press, Cambridge, Massachusetts, U.S.A.

Limpert, R. (1975). "Cooling analysis of disc brake rotors". *Truck Meeting Philadelphia, Pa. November 10-13. SAE Technical Paper 971014*.

Naji, M. and M. AL-Nimr (2001). "Dynamic thermal behavior of a brake system". *Int. Comm. Heat Mass Transfer* **28**:6, pp. 835–845.

Nisonger, R. L., C.-h. Yen, and D. Antanaitis (2011). "High temperature brake cooling - characterization for brake system modeling in race track and high energy driving conditions". *SAE Int. J. Passeng. Cars - Mech. Syst. SAE Technical Paper 2011-01-0566* **4**, pp. 384–398.

optris CTlaser LT/1M/2M/3M/G5. optris.

Rajamani, R. (2006). *Vehicle Dynamics and Control*. Springer Science+Business Media, Inc, 233 Spring Street, New York, NY 10013, USA.

Schopper, A. (2008). *Thermophysical Properties of 2 Metal Samples*. Tech. rep. Applications Laboratory Thermophysical Properties Section.

Shen, F. Z., D. Mukutmoni, K. Thorington, and J. Whaite (1997). "Computational flow analysis of brake cooling." *SAE Technical Paper 971039*, pp. 95–106.

Sheridan, D. C., J. A. Kutchey, and F. Samie (1988). "Approaches to the thermal modeling of disc brakes". *SAE Technical Paper 880256*.

Talati, F. and S. Jalalifar (2009). "Analysis of heat conduction in a disk brake system". *Heat Mass Transfer* **45**, pp. 1047–1059.

Vehicle Regulations UN ECE-R13 (2008). `http://www.unece.org/fileadmin/DAM/trans/main/wp29/wp29regs/r013r6e.pdf`. United Nation Economic Commission for Europe.

Lund University
Department of Automatic Control
Box 118
SE-221 00 Lund Sweden

Document name
MASTER´S THESIS

Date of issue
June 2015

Document Number
ISRN LUTFD2/TFRT--5966--SE

Author(s)
Sofia Finnved
Sebastian Nöbbelin

Supervisor
Rolf Johansson, Dept. of Automatic Control, Lund University, Sweden
Karl-Erik Årzén, Dept. of Automatic Control, Lund University, Sweden (examiner)

Sponsoring organization

Title and subtitle
Temperature Estimation in Trailer Disc Brake

Abstract

Automatic brake functions in trucks and cars can save lives but may heat the brakes to dangerous temperature levels. Various types of models for temperature estimation in a disc brake have been evaluated. A homogeneous temperature inside the disc was assumed and this simplification gave adequate modeling results. The implementation was done in Simulink.

One model estimated the heat generation based on the kinetic energy difference during a brake event. The difficulty of estimating driving resistance coefficients and the sensitivity to the driver's behavior made this model less suitable for generalization. More promising models used the brake cylinder pressure as input. The brake cylinder pressure was used to derive a braking force at the periphery of each wheel. The braking force could be determined in different ways, each one with their own advantages and disadvantages. The common disadvantage was that the brake force depends on the load over each wheel. It was assumed that the load over each wheel be known. A simple, exponential model for cooling gave sufficiently good results. A model based on the sum of convection and radiation gave better results.

The brake pressure model was used in a short study on steady state temperatures, while the vehicle was pulse braked. No conclusions was drawn from these simulations, but the results were promising, thus opening up for future research.

Keywords

Classification system and/or index terms (if any)

Supplementary bibliographical information

ISSN and key title
0280-5316

ISBN

Language
English

Number of pages
1-59

Recipient's notes

Security classification